UNIVERSIDADE FEDERAL DE SANTA CATARINA
CENTRO DE CIÊNCIAS DA SAÚDE
PROGRAMA DE PÓS-GRADUAÇÃO EM ODONTOLOGIA
MESTRADO EM IMPLANTODONTIA

MARÍA ELISA GALÁRRAGA VINUEZA

SÍNTESE, CARACTERIZAÇÃO E CAPACIDADE DE INIBIÇÃO DE BIOFILME POR BIOVIDRO ATIVO 58S ATRAVÉS DA INCORPORAÇÃO DE COMPOSTOS ORGÂNICOS E INORGÂNICOS

Dissertação de Mestrado

Orientador: Prof. Dr. Ricardo de Souza Magini
Co-orientador: Prof. Dr. Júlio César Matias de Souza

Florianópolis
2017

María Elisa Galárraga Vinueza

SÍNTESE, CARACTERIZAÇÃO E CAPACIDADE DE INIBIÇÃO DE BIOFILME POR BIOVIDRO ATIVO 58S ATRAVÉS DA INCORPORAÇÃO DE COMPOSTOS ORGÂNICOS E INORGÂNICOS

Dissertação submetida ao Programa de Pós-Graduação da Universidade Federal de Santa Catarina para a obtenção do Grau de Mestre em Odontologia na área de concentração de Implantodontia.
Orientador: Prof. Dr. Ricardo de Souza Magini
Coorientador: Profª. Dr. Júlio César Matias de Souza

Florianópolis
2017

María Elisa Galárraga Vinueza

SÍNTESE, CARACTERIZAÇÃO E CAPACIDADE DE INIBIÇÃO DE BIOFILME POR BIOVIDRO ATIVO 58S ATRAVÉS DA INCORPORAÇÃO DE COMPOSTOS ORGÂNICOS E INORGÂNICOS
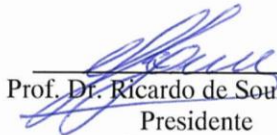
Esta Dissertação foi julgada adequada para obtenção do Título de "Mestre em Odontologia", e aprovada em sua forma final pelo Programa de Pós-Graduação em Odontologia.

Florianópolis, 26 de maio de 2017.

Profª. Drª. Elena Riet Correa Rivero
Coordenadora do Curso

Banca Examinadora:
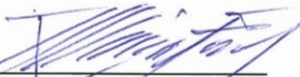
Prof. Dr. Ricardo de Souza Magini
Presidente
Universidade Federal de Santa Catarina

Profa. Dra. Ariadne Cristiane Cabral da Cruz
Universidade Federal de Santa Catarina

Prof. Dr. César Augusto Magalhães Benfatti
Universidade Federal de Santa Catarina

Prof. Dr. Márcio Celso Fredel
Universidade Federal de Santa Catarina

Este trabajo está dedicado al infinito amor y fe que tengo por Dios, con Él y en Él somos la herramienta para mejorar este mundo.

AGRADECIMENTOS

Realmente é impossível descrever todo meu agradecimento com palavras. O sentimento com certeza é muito mais forte do que esta página pode transmitir...

En primer lugar quiero agradecer a DIOS por iluminar cada día de mis 26 años de vida. Gracias SEÑOR por darme tanto, por amarme, por hacerme sentir enamorada de esta vida, gracias por bendecirme con una familia tan maravillosa, gracias por darme amigos que son tesoros inigualables, gracias por darme acceso al conocimiento y a la ciencia, gracias por colocar en mi vida a mis profesores que me han hecho descubrir tu infinito mundo y querer ser mejor cada día. GRACIAS por ser mi razón de vivir. Esta vida no podría ser mejor.

A mis papás, no puedo ni explicar el amor y agradecimiento que siento por ustedes. Me han hecho sentir amada desde que fui una pequeña célula. Ustedes me esperaron con tanta esperanza llenando mi espíritu con esa ilusión, lo cual hasta el día de hoy me hace saber que en esta vida tengo un propósito, una razón de ser. **Mamá**, eres todo lo que quiero llegar a ser. Gracias por enseñarme desde la primera vez que me tuviste en tus brazos que debía amar, cuidar y cultivar mi cuerpo porque es el templo de DIOS. Gracias por tu mirada llena de fuerza y energía que me enseña día a día a amar incondicionalmente, a ser perseverante, a luchar por mis ideales, a creer en mí. **Papá**, mi ejemplo a seguir. Gracias por tu infinito amor, tu hermosa sonrisa que alegra mis días. Tu energía puede atravesar cualquier barrera, desde el corazón más duro hasta el más blando. Tú me enseñaste a llegar al corazón de las personas con un saludo, un abrazo, una sonrisa. Tú me enseñaste a esperar lo mejor de todas las personas y a intentar ser la mejor versión de mí misma para ser un excelente ser humano antes que cualquier logro académico o profesional. Gracias por iluminar ni corazón con tu amor y alegría, pienso en ti y sonrió todos los días. **Hermana**, quien tiene la otra parte de mi corazón. Tú le pediste a Dios que llegue a este mundo. Llegué para ser tu compañera, tu hombro, tu mano derecha, tu respaldo. Tienes el corazón más puro que he conocido, del cual intento aprender cada día para ser más bondadosa y generosa. Nuestros corazones están unidos, siempre juntas para enfrentar cualquier adversidad. Gracias por ser la mejor hermana del mundo y protegerme.

Prezados professores, obrigada por todo seu exemplo e ensino. É um orgulho para mi ser sua aluna. **Professor Magini** obrigada por ser meu orientador, por ser a pessoa que sempre sabe como motivar-me no momento exato. Tanto eu como meu pai sentimos seu carinho a primeira

vez que entramos no CEPID. O professor me deu a benvinda no Brasil, desde o começo eu soube que um largo caminho de aprendizagem me esperava do seu lado. **Professor César**, obrigada por ser um exemplo de paixão pelo ensino, é um professor que me inspira e motiva para querer ser professora num futuro. Obrigada por sempre cuidar de todos seus alunos no CEPID. Você faz que todos nos sintamos numa família. **Professor Bianchini**, obrigada por seu constante ensino dia a dia na clínica, na pesquisa e na vida. Obrigada pela sinceridade, o professor me ensinou a procurar o caminho da excelência, a tentar dar o melhor de mim e tomar uma postura mais forte na vida. Cada dia eu fico mais inspirada para continuar pesquisando com o professor. **Professor Cardoso**, obrigada por ser meu orientador espiritual. Por ensinar para mim semana traz semana a palavra do nosso CRIADOR. Obrigada, por ser meu exemplo de humildade, sabedoria e equilíbrio. O professor foi um apoio inigualável no Brasil, obrigada por todo seu carinho. **Professor Fredel**, obrigada por seu apoio e carinho na minha pesquisa, o professor foi um pilar fundamental para mim**. Professor Júlio**, obrigada por sua co-orientação e apoio, sempre esteve do meu lado no meu mestrado.

Obrigada a meus colegas, **Adri** por ser mi hermana en Brasil y tener un corazón tan grande y transparente que nunca se cansa de hacer feliz a los demás. **Karin**, gracias por tu apoyo, bondad, eres una amiga increíble que me enseña cada día. **Edwin**, gracias por siempre estar a mi lado, apoyándome con tu radiante energía que siempre me da fuerza. **Nicolás**, gracias por tu nobleza, tu corazón gigante y por siempre estar dispuesto a ayudarme y cuidarme.

Carol Morsch, obrigada por entrar na minha vida, você é um exemplo de integridade para todos, sempre quero seguir teu exemplo. Sua amizade é um presente de Deus. **Mari**, obrigada por tua pureza, sinceridade, por teu olhar cheio de amor que sempre me dá alegria e me lembra que neste mundo existem pessoas inigualáveis como você. **Renata**, minha dupla, nós aprendemos tanto juntas. Espero continuar aprendendo a vida inteira com você. Obrigada por sua amizade, você é uma amiga incondicional que me ensina que devemos lutar por nossos desejos. A todos os colegas do CEPID, Nathi, Paty, Miguel, Artur, Gaby, Bruna, Gabriel, Juan, Suzeli, Rafa, e Sil, obrigada por sua amizade e por sua generosidade de tempo, conhecimento e carinho. Vocês são um presente de Deus na minha vida.

"E não vos conformeis com este mundo, mas transformai-vos pela renovação do vosso entendimento, para que experimenteis qual seja a boa, agradável e perfeita vontade de Deus."

Romanos 12:2

RESUMO

O biovidro ativo é um biomaterial promissor que tem mostrado excelentes efeitos osteogênicos, angiogênicos e antibacterianos para ser aplicado em procedimentos de reparação óssea em diversas áreas. Em implantologia oral, infecções podem ocorrer após procedimentos cirúrgicos em decorrência da presença de biofilmes orais incluindo espécies patogênicas. Sendo assim, este trabalho teve como principal objetivo desenvolver biomateriais à base de um biovidro nano-estruturado para incorporação de compostos com potencial anti-biofilme. O biovidro ativo 58S foi modificado incorporando brometo, compostos derivados do cranberry e da própolis na sua estrutura. As amostras foram caracterizadas por meio de análise química, textural e física. O potencial anti-biofime do biovidro ativo foi determinado através de q-PCR e análise microscópico. A reatividade química foi avaliada por meio de análise química, microscópica e da proporção Ca/P. As amostras do biovidro ativo incorporando brometo, cranberry PACS e própolis mostraram uma distribuição de tamanho de partículas, estrutura física e composição química apropriadas. O biovidro ativo modificado com 5wt% $CaBr_2$ inibiu a proliferação de *S. mitis, V. parvula, P. gingivais, S.gordoni, A. viscosus,* e *F. Nucleatum.* Uma significativa formação de hidroxiapatita carbonatada foi revelada nas amotras do biovidro ativo mesoporoso incorporando cranberry PACS e própolis após 72 h de imersão na solução corporal simulada. Por conseguinte, a incorporação de compostos inorgânicos e orgânicos no biovidro ativo 58S pode ser uma estratégia para potencializar seu efeito anti-biofilme e ser aplicado em tratamentos de reparo e infecção óssea.

Palavras-chave: 1. Biovidro ativo 2. Antibiofilmes 3. Enxerto ósseo 4. Sínteses sol-gel 5. Infeção óssea 6. Reparo ósseo

ABSTRACT

Bioactive glass is an attractive biomaterial that has shown excellent osteogenic, angiogenic and antibacterial effects for bone healing. One of the main issues regarding oral surgery and bone grafting procedures are the recurrent infections caused by oral biofilm involving pathogenic species. Thus, the main aim of the present study was to produce porous bioactive glasses incorporating inorganic and organic compounds in their chemical and physical structure to enhance anti-biofilm potential during bone repairing procedures. The modified 58S bioactive glasses embedded bromide, cranberry PACS and propolis compounds and were characterized through physical, chemical and textural analysis. Bioactive glass multispecies antibiofilm potential was evaluated by q-PCR analysis and microscopic observation. Chemical reactivity of the samples was examined through chemical, microscopic and Ca/P ratio analysis. Bioactive glasses embedding bromide, cranberry PACS and propolis showed an appropriate particle size distribution, chemical and physical properties. Bioactive glass embedding 5wt% $CaBr_2$ inhibited *S. mitis, V. parvula, P. gingivais, S.gordoni, A. viscosus,* and *F. nucleatum* proliferation. A significant hydroxyl-carbonate apatite layer was revealed by mesoporous BG samples incorporating cranberry PACS and propolis compounds after immersion in simulated body fuid for 72 h. The incorporation of inorganic and organic compounds into bioactive glass structure can be a strategy to enhance its antibiofilm potential for bone healing and infection treatment procedures.

LISTA DE FIGURAS

Figuras Artigo 1

Figuras Artigo 2

Figuras Artigo 3

LISTA DE TABELAS

Artigo 1

Artigo 3

LISTA DE ABREVIATURAS E SIGLAS

BET	Método Brunaeur-Emmet-Teller
BJH	Método Barrett-Joyner-Halenda
BG	Biovidro ativo
EDX	Espectroscopia de Energia Dispersiva
EPS	Sustâncias poliméricas extracelulares
FTIR	Espectroscopia no infravermelho por transformação de Fourier
CHA	Hidroxiapatita carbonatada
CaBr2	Brometo de Cálcio
MBG	Biovidro Mesoporoso
MEC	Matriz extracelular
MEV	Microscopia eletrônica de varredura
Min	Minutos
MTS	[3-(4,5-dimethylthiazol-2-yl)-5-(3-carboxymethoxyphenyl)-2-(4-sulfophenyl)-2H-tetrazolium
NPs	Nano partículas
PBS	Solução tampão de fosfato
pH	Potencial hidrogeniônico
OS	Solução de penicilina/estreptomicina
q-PCR	Reação em cadeia da polimerase quantitativa
Ra	Rugosidade média
Rt	Rugosidade total
ROG	Regeneração óssea guiada
SBF	Solução corporal simulado
SEM	Microscopia Eletrônica de Varredura
XRD	Difração de raios X

SUMÁRIO

CAPÍTULO I

1 INTRODUÇÃO

No ano 2012, foi estimado que nos Estados Unidos mais de meio milhão de pacientes foram submetidos a cirurgias de enxerto ósseo por ano, representando um custo acima de 2,5 bilhões de dólares anuais. Espera-se que para o ano 2020 este número de pacientes seja o dobro devido ao aumento de expectativa de vida da população mundial (AMINI; LAURENCIN; NUKAVARAPU, 2012). Além do referido, o osso é o segundo tecido mais transplantado no mundo depois do sangue (JONES, 2013).

Em decorrência do mencionado, a engenharia tecidual se encontra constantemente pressionada pela extensa demanda de cirurgias de enxertia óssea. Na área bucal e maxilofacial, procedimentos de enxerto ósseo para o reparo e regeneração dos tecidos são utilizados frequentemente. Por conseguinte, a procura para desenvolver um biomaterial ''ideal'' para substituir os tecidos ósseos é um tema de grande interesse e vários anos de pesquisa.

Atualmente, os enxertos de origem autógena removidos de um leito doador do próprio paciente, são considerados o ''padrão ouro'' da enxertia por ter as características desejadas de osteoindução e osteocondução. No entanto, a alta demanda de procedimentos de enxertia na região oral dificulta a utilização de osso de origem autógena de todos os enxertos devido a fatores limitantes como a necessidade de uma área doadora com um volume apropriado, envolvimento de um procedimento cirúrgico adicional e aumento da morbidade do paciente por ser submetido a um maior número de intervenções. Por outro lado, os aloenxertos, removidos e transplantados entre indivíduos de uma mesma espécie com características genéticas diferentes, já foram mais utilizados no passado. Atualmente são conhecidas desvantagens como a reabsorção precoce, potencial de transmissão de proteínas antigênicas e doenças infecciosas e a necessidade de um banco de ossos. Por este motivo, a engenharia tecidual tem desenvolvido por vários anos diversos materiais metálicos, cerâmicos e poliméricos a fim de substituir os tecidos ósseos perdidos, considerando que a utilização desses materiais depende de propriedades essenciais como a biocompatibilidade, bioatividade, estabilidade física e química e propriedades mecânicas similares aos tecidos perdidos. Assim, os principais materiais aloplásticos cerâmicos que têm sido desenvolvidos a fim de ter as características mencionadas são a hidroxiapatita, o beta fosfato tricálcio, o fosfato de cálcio bifásico e os biovidros ativos (CRUZ et al., 2006). No entanto a procura do biomaterial ''ideal'' para substituir o tecido

ósseo é um constante desafio que a engenharia tecidual enfrenta atualmente, já que ainda não existe um biomaterial com as propriedades biológicas do tecido autógeno e que contenha biomoléculas capazes de induzir a formação óssea (JONES, 2013).

Além dos fatores biológicos, químicos e mecânicos de um biomaterial "ideal", a capacidade antibacteriana e antibiofilme é uma característica adicional desejada e requerida nos procedimentos de enxertia óssea. A incidência de infecção óssea pós-operatória é considerável e é uma complicação frequente das cirurgias orais envolvendo enxertia óssea (EL-KADY et al., 2012b; XIE et al., 2009). As bactérias organizadas no biofilme são as protagonistas de 80% das infecções humanas (DAVIES, 2003). De modo que a utilização de antibiótico terapia é frequente para a prevenção de infecções secundárias neste tipo de procedimentos, no entanto o antibiótico não é sempre capaz de induzir um efeito efetivo no tecido ósseo infectado já que não atua de forma local e atua em uma área com pouca vascularização. Adicionalmente, as bactérias organizadas em biofilme são mil vezes mais resistentes ao antibiótico comparadas com as bactérias planctônicas (DAVIES, 2003; GALARRAGA-VINUEZA et al., 2017). Assim, um biomaterial com propriedades antibiofilme seria capaz de atuar de maneira mais eficaz e local na área enxertada infectada. No entanto, poucos materiais têm demostrado capacidade antibacteriana e antibiofilme consistente.

O biovidro ativo desenvolvido no ano 1969, aplicado em mais de um milhão de pacientes no mundo para procedimentos de regeneração óssea (HOPPE; GÜLDAL; BOCCACCINI, 2011; JONES, 2013), é um biomaterial capaz de inibir o crescimento bacteriano através da liberação de íons que elevam o pH do meio e criam um ambiente pouco favorável para o crescimento bacteriano (ALLAN; NEWMAN; WILSON, 2002; KRISHNAN; LAKSHMI, 2013). Esta característica ambiciosa do biovidro, além das suas outras propriedades de promover a osteogênese e angiogênese tem posicionado o biovidro ativo como um biomaterial promissor (JONES, 2013). Certamente, a capacidade antibacteriana do biovidro ativo é de fundamental importância por ter um efeito local desejado no leito cirúrgico (BELLANTONE; COLEMAN; HENCH, 2000; HENCH, 2006). Entretanto, o efeito antibiofilme dos biovidros ativos não foi elucidado nem confirmado nos últimos estudos (GALARRAGA-VINUEZA et al., 2016), razão pela qual diversas pesquisas têm mudado a composição e a estrutura do biovidro ativo a fim de conseguir uma maior capacidade antibacteriana e antibiofilme (HUM; BOCCACCINI, 2012). Diferentes avanços têm sido

apresentados como a incorporação de agentes antibacterianos na composição química ou estrutura física do biovidro ativo. Deste modo, compostos de prata, céria, selênio, flúor, entre outros têm sido adicionados na fórmula química do biovidro ativo a fim de melhorar sua capacidade antibacteriana e antibiofilme (MALAVASI et al., 2012; STEVANOVIĆ et al., 2015; XU et al., 2015). Por outro lado, a tecnologia nano tem mudado a estrutura deste material adicionando surfactantes (XIA; CHANG, 2006) na sua fórmula para induzir a formação de poros convertendo assim o material num biovidro ativo mesoporoso que tem a capacidade de incorporar nos seus nano poros substâncias antibacterianas e antibiofilmes como antibióticos, nano partículas bioativas e compostos naturais orgânicos (EL-GHANNAM; AHMED; OMRAN, 2005; JIA et al., 2010; PRABHU et al., 2014; XIA et al., 2008).

Considerando que ainda não existe um consenso, assim como estudos suficientes esclarecendo que tipo de compostos têm efeito antibiofilme, o objetivo do presente estudo foi desenvolver e avaliar a capacidade antibiofilme do biovidro ativo 58S incorporando compostos orgânicos e inorgânicos na sua estrutura química e física. De tal modo, a hipótese do presente estudo é que a incorporação de agentes inorgânicos e orgânicos no biovidro ativo potencializará seu efeito inibitório do biofilme oral.

Por conseguinte, o presente manuscrito está dividido em três partes, sendo a primeira uma revisão da literatura da incorporação de agentes antibacterianos e antibiofilmes no biovidro ativo, a segunda descrevendo a capacidade antibiofilme do biovidro ativo modificado com brometo de cálcio e a terceira mostrando o desenvolvimento e bioatividade do biovidro ativo mesoporoso incorporando compostos de origem natural.

CAPÍTULO II

2 ARTIGO 1 EM INGLÊS

O artigo a seguir foi publicado na revista científica *Journal of Biomedical materials research: part A*. Fator de impacto: 3.263. Qualis: A1

Anti-biofilm properties of bioactive glasses embedding organic active compounds

M.E. Galarraga-Vinueza[1], J. Mesquita-Guimarães[2], R. S. Magini[1], J. C. M. Souza[1,2], M. C. Fredel[2], A. R. Boccaccini[3*]

[1]Center for Education and Research on Dental Implants (CEPID), Post-Graduation Program in Dentistry (PPGO), Department of Dentistry (ODT), Federal University of Santa Catarina(UFSC), Florianópolis/SC, 88040-900, Brazil
[2]Ceramic and Composite Materials Research Group (CERMAT), Federal University of Santa Catarina, Florianópolis 88040-900, Brazil
[3]Institute of Biomaterials, Department of Materials Science and Engineering, University of Erlangen-Nuremberg, 91058 Erlangen, Germany

*Corresponding author: A.R. Boccaccini, aldo.boccaccini@ww.uni-erlangen.de

Abstract:
Bioactive glasses (BGs) are promising materials for bone repair due to their desirable properties such as osteoconductivity, biodegradability, angiogenic potential, and antibacterial activity. Ionic dissolution products from bioactive glasses increase the medium pH inhibiting surrounding bacteria proliferation. The activity of BGs against biofilm formation has been enhanced by incorporating organic antibacterial compounds. The aim of this review was to summarize evidence in literature which assesses the efficacy of antibacterial and anti-biofilm compounds embedded in bioactive glasses to prevent peri-implant infection during bone healing. A PubMed bibliographical research was carried out including articles published in the last 20 years. Most previous studies evaluated antibacterial efficiency in planktonic cultures but did not investigate biofilm inhibition, underestimating biofilm clinical relevance. Multifactorial features such as biocompatibility of embedded compounds, receptor site characteristics, and drug delivery

efficiency have been found to influence the bioactive glass capability of acting both as an anti-biofilm agent and as a bone repairing biomaterial. Accordingly, further in vitro and in vivo studies are required to select the most promising anti-biofilm agents which should be incorporated into bioactive glasses to counteract biofilm proliferation, without inducing toxic effects on human cells, and with the added functionality of promoting bone regeneration.

Key Words: bioactive glass, mesoporous materials, antibacterial compounds, anti-biofilm activity, drug delivery system

2.1 INTRODUCTION

Bone is the second most transplanted tissue in surgical procedures worldwide with bone tissue engineering being investigated as a realistic alternative for bone healing [1]. Bone tissue engineering often relies on an engineered scaffold acting as a temporary extracellular matrix to support and deliver cells [2]. Bioactive glasses (BGs) involve a group of inorganic biomaterials discovered in the late 1960s that have been applied in bone repair due to their bioactivity, osteogenic, and angiogenic potential, biodegradability, and osteoconductivity [3]. BGs stimulate diverse biologic responses in contact with physiological fluids, such as the development of a carbonated hydroxyl-apatite (CHA) surface layer that is comparable to the mineral phase of bone and acts as an interface to enhance the attachment of bone cells. BGs also possess antibacterial potential due to their high surface reactivity and ion release capability [4, 5] causing high aqueous pH values in the surrounding tissues; however, such antibacterial effect has been reported to be restricted to certain planktonic bacteria [6–11]. Consequently, various approaches have been put forward for the incorporation of additional antibacterial compounds into BG compositions to enhance antibacterial and anti-biofilm activity, this being the subject of the present review.

Biofilm is a multi-species agglomerate of microbial cells enclosed in a well-organized extracellular polymeric substance (EPS) matrix that adheres to soft and hard surfaces. The EPS matrix allows genetic information exchange and chemical signaling between microbial cells through a mechanism known as quorum sensing. Biofilms act as a biological barrier against therapeutic agents and host immune cells; retaining also nutrients from the environment [12,14]. Biofilms containing pathogenic species are reported to cause over 80% of human infections [12–14]. Oral biofilms adhere to different surfaces of prostheses, implants, mucosa, teeth, and bone. Biofilm formation is a

gradual process consisting of four distinct stages [13–15]: (a) acquired pellicle formation; (b) primary (early) colonization; (c) secondary colonization/ co-aggregation; and (d) mature biofilm establishment. The early colonization begins through binding primary bacteria to a conditioning film composed of glycoproteins, water and nutrients, that is previously established in the mouth. The first adherent oral bacteria (Streptococcus sanguinis, S. oralis, S. gordonii, S. mitis, Actinomyces naeslundii, Capnocytophagaochraceae, S. mutans and S. sobrinus) are weakly and reversibly linked to glycoproteins named by adhesins, although they may remain and proliferate, starting the phenomena of microbial co-aggregation. Steptococcus species represent 60–80% of all primary colonizers. Such coaggregation is mediated by metabolic and genetic exchange known as quorum sensing. The secondary colonization occurs within 3–5 days after the beginning of the early colonization. In this process, the microorganisms start to multiply and to co-aggregate with partner species leading to the biofilm structural organization. Microorganisms organized in biofilms achieve a strong adherence to oral surfaces leading to a maturation process within 2–3 weeks [12–15].

Previous studies have described that biofilms are about one thousand times more resistant to antibiotic therapy compared to free floating planktonic bacteria [12, 15]. In addition, studies have described that conventional systemic antibiotic therapy is not as effective as expected to eradicate bone infection because antibiotics do not act locally in septic areas and they may induce side effects in patients [13,16]. In the last decade, sol-gel derived mesoporous bioactive glasses (MBGs) have been developed with the purpose of becoming carriers for therapeutic agents acting as drug delivery systems [17–20]. Consequently, MBGs are advantageous candidates for both bone repair and peri-implant infection treatment since they combine unique properties to stimulate bone growth and prevent bacteria proliferation.

The present review assesses antibacterial and antibiofilm efficacy of BG carriers embedding organic compounds focusing on multifactorial parameters that can control antibacterial effects during bone healing. A PubMed electronic search including articles published in the last 20 years was performed using the following combination of key words and MeSH terms: "bioactive glass" or "Bioglass" and "antibacterial" or "anti-infective" or "antibiotics" or "antibacterial" or "biofilm inhibition". The selection criteria identified papers describing in vitro and in vivo studies, thus only articles that evaluated specifically antibacterial or anti-biofilm effects of bioactive glasses embedding antibacterial compounds were reviewed and discussed. The present

article is not intended to be comprehensive in terms of the number of studies included; it is rather a discussion article containing the relevant information found in key publications to provide the reader with initial points for further analysis.

2.2 ORGANIC AGENTS INCORPORATED INTO BIOACTIVE GLASS

In the last years, several studies have shown proper antibacterial properties achieved by different formulations of bioactive glasses incorporating several oxides [21–23] and the effects of biologically active ions on bone tissue engineering have been discussed in literature [24]. In addition, commercial products based on bioactive glass (melt-derived, composition SiO_2 53%, Na_2O 23%, CaO 20%, P_2O_5 4%) are being successfully applied in the clinic to treat osteomyelitis [25] and the application of BGs to treat bone infections by the effect of pH increase is well demonstrated in literature [4,6,26,27]. Recent studies describe the incorporation of triclosan 28 into BG considering that this compound has already been applied in mouthwash solutions for clinical considerations involving biofilm-induced infections. Xu et al. reported in vitro antibacterial effects of 45S5 BG embedding triclosan against cariogenic *S. mutans* biofilm [29]. This study assessed anti-biofilm activity by pouring BG powders incorporating triclosan into wells containing S. mutans biofilm plaques that had undergone 6, 12, and 24 h of growth conditions. After 10 min of exposure, each coverslip containing biofilm was washed with PBS and centrifuged in saline solution. Subsequently, *S. mutans* biofilm was detached from the cover slips and then incubated in agar plates for 48 h at 37∘C, simulating oral conditions. Biofilm viable colonies were counted and observed using a stereomicroscope and scanning electron microscope. The study showed additive anti-biofilm effects when BG was combined with triclosan. Pertinently, this previous study focused on the assessment of anti-biofilm activity rather than antibacterial effect against planktonic cultures. However, this broad-spectrum antibacterial agent is hydrophobic and can accumulate in human fatty tissues, breast milk, urine, and serum [30]. Furthermore, that synthetic organic agent has been reported to cause endocrine disruption in mammals, affecting the thyroid hormone reproduction and its homeostasis, [31] so that further research on triclosan containing BGs will have to investigate possible negative effect of its use.

Natural organic compounds derived from medicinal plants known as phytotherapeutics can promote both antibacterial and anti-inflammatory activity [32]. The scientific interest in natural active compounds has increased for biomedical applications, since they are well-known health-promoting agents and produce minimum side effects. Essential oils derived from plants have numerous desirable properties being antibacterial, antiviral, antifungal, and having insecticide potential [33]. Regarding natural organic compounds as favorable antibacterial agents in combination with BGs, Prahbu et al. [34] studied the in vitro antimicrobial effect of BGs of composition ($58SiO_2$-$33CaO$-$9P_2O_5$) incorporating neem plant (*Azadirachta indica*) leaf powder, a natural antiviral and antibacterial compound against a broad spectrum of bacteria [35]. BG nanoparticles (NPs) doped with neems leaf powder were analyzed by using Kirby-Bauer disc diffusion method and exhibited considerable antimicrobial activity against *S. aureus* and *E. coli* cultures. Additionally, neem doped BG NPs demonstrated superior antibacterial properties against Gram-positive and Gram-negative bacteria in comparison to those recorded for silver doped or pure BG NPs. Besides the beneficial antibacterial effect, neem-doped BG nanoparticles were analyzed by MTT assay and exhibited reduced cytotoxic effects. Results of that study established that neem doped BG was a biocompatible and potent antibiofilm agent for tissue engineering applications [34].

An alternatiive approach toward incorporating natural organic compounds into BGs was performed by Bonfim et al. [36]. In this study, Brazilian red and green propolis were incorporated into BGs of composition $(SiO_2)0.80(P_2O_5)0.04(CaO)0.16$. Propolis, a natural non-toxic beehive agent found in honeycombs, has antifungal and antiviral properties as well as antibacterial activity against a wide range of cocci and Gram-negative rods [37]. Propolis solution was added during the BG sol-gel synthesis to obtain specimens for antimicrobial assays. The in vitro study reported growth inhibition on the following pathogenic species: *S. aureus, E. faecalis, S. mutans, P. intermedia, F. nucleatum, P. gingivalis,* and *A. actinomycetemcomitans* [36]. Accordingly, propolis is considered an antibacterial natural compound of high potential for future developments given its ability to inhibit bacterial adherence, prevent biofilm accumulation, and to reduce virulence factors of *S. mutans* [38]. Also, Propolis has been evaluated in previous studies showing a noncytotoxic nature [39, 40]. Grenho et al. [41] reported that propolis had antibacterial effectiveness and exhibited bioactive

characteristics such as stimulation of fibroblast migration, high cell metabolic activity, and absence of cell membrane damage.

Despite the success reported by some investigations mentioned above, organic compounds, especially natural derived agents like phytotherapeutics have not been largely explored to date in combination with BGs. Since BGs have the ability to incorporate both hydrophilic and hydrophobic groups in their structures, in vitro and in vivo studies involving natural organic compounds bound to BGs are expected to increase. Considering that various nature derived agents have reduced or non-cytotoxic effects [32–34,40] future investigations involving also clinical trials should be performed to identify the advantages and synergies brought by the combination of natural organic compounds and BGs to avoid peri-implant infections.

2.3 BIOACTIVE GLASS AS AN ANTIBIOTIC DELIVERY SYSTEM

In the last 15 years, BGs have been increasingly considered as vehicles for the local delivery of drugs, growth factors, and antibiotics [17–19, 42–45]. Tissue engineering approaches using BG scaffolds, which include a therapeutic drug or antibiotic delivery capability are based on multifunctional scaffolds, which are capable of releasing therapeutic substances against microbial infections in a controlled manner during the process of tissue repair [17, 42, 43, 45–48]. Systemic antibiotic therapy is not always effective to treat bone infections since there is vascular insufficiency and antibiotics may not arrive to infected areas through the blood stream. On systemic therapy, antibiotic biomolecules can be inactivated in the blood stream and may have no effect where they are needed at the implanted sites [8, 17]. In cases of bone repair procedures, there is a high incidence of infection and inflammatory response caused by host immune reactions. Attempting to solve implantation site complications, BG carriers with well-organized mesoporous structures are developed [18–20, 44, 45] which exhibit adjustable pore diameter and high surface area where antibiotics can be encapsulated for their controlled delivery. A previous study involving MBG reported a continuous release of gentamicin for six days inhibiting bacterial adhesion and biofilm formation of S. aureus and S. epidermis, which are prevalent species at implant infections [44].

Similarly, Xie et al. [46] preformed an in vivo study to evaluate the antibacterial effect of loaded gentamicin pellets composed of chitosan and borate-based BG. A bone tissue infection (osteomyelitis)

associated to Gram-negative bacilli was induced in a rabbit tibia model and then treated by the application of gentamicin-loaded BG pellets. Results from microbiological, radiographical, and histological assays stated an eradication of 81.82% infected cases. That study indicated that gentamicin-loaded BG pellets are attractive materials for osteomyelitis treatment. In addition, related in vivo studies performed by Nandi et al.[47] reported control of bone resorption in experimental osteomyelitis and consequent formation of lamellar bone by using cefuroxime axetil (CFA)-loaded MBG.

The results of several studies have thus indicated that local antibiotic release from MBGs can be a solution to treat bone infection. Various antibiotics such as carbeinicillin, [48] ciprofloxacin, [49] tetracycline hydrochloride (TCH), [50,51] vancomycin, [52,53] and teicoplanin [54] have been incorporated into BGs, as summarized in Table I. Nevertheless, biofilm infections at receptor sites are resistant to several antibiotics due to the presence of pathogenic species in well-organized extracellular matrices [12]. Rastegar et al. [55] reported that *P. aureginosa*, a specie associated to the formation of biofilm on implanted devices, was resistant to carbenicillin, cotrimoxazole, ceftizoxime, gentamicin, and tetracycline in 95% of the cases of wound infections. On a comparative study of antibiotic resistance between planktonic bacteria and biofilm cultures, Olson et al. [13] found that the minimum biofilm inhibitory concentrations of cloxacillin, amoxicillin, gentamicin, ampicillin, tetracycline, penicillin G, and ceftiofur were not able to eradicate biofilms formed by *A. pyogenes, S. aureus, S. hyicus, S. agalactiae, C. renale,* and *C. pseudotuberculosis*. However, it was shown that planktonic cultures were susceptible to several antibiotics. Considering the clinical relevance of biofilm resistance to antibiotics, incorporating anti-biofilm compounds rather than antibiotics into BGs represents a more effective approach that should be explored more intensively in future. Further studies are required to understand and characterize factors involved in biofilm growth, microbial gene exchange, and bacteria communication to develop new anti-infective chemotherapies, which can involve BGs loaded with antibiofilm agents.

Table I. Summary of Relevant Studies on Antibiotic-Loaded Bioactive Glasses to Prevent Infection

Study/ Experimental design	BG composition	Loaded Antibiotic	Outcome	
			Antibacterial Effect	Targeted bacterias
Li et al. (LI et al., 2013) *In vitro*	Mesoporous BG *	Gentamicin	Inhibition of bacterial adhesion and biofilm formation	S. *aureus* S. *epidermis*
Xie et al. (XIE et al., 2009a) ***In vitro/ in vivo (osteomyelitis induced in an animal model)***	Pellets of chitosan-bonded with borate BG [mol%] 6Na$_2$O,8K$_2$O, 8 MgO, 22 CaO, 54 B$_2$O$_3$, 2P$_2$O$_5$	Gentamicin	***In vitro*:** Inhibition of bacterial growth ***In vivo:*** 6 weeks after implantation, 9 out of 11 rabbits were negative for E. coli by culture analysis. Eradication of 81.82% of bone infection cases demonstrated by radiographic, histopathologic, and microbiological examinations.	E. *coli*
Miola et al. (MIOLA et al., 2013) ***In vitro***	BG [mol%] 45SiO2,3P2O5, 26CaO, 7MgO, 15Na2O, 4K2O	Carbenicillin	Samples released an antibiotic amount considerably higher than S. *aureus* MIC (minimum inhibitory concentration) of carbenicillin.	N.A.
Mabrouk et al. (MABROUK et al., 2014) ***In vitro***	Composite scaffolds of polyvinyl alcohol and quaternary 46S6 BG [mol%] 46SiO$_2$, 24 CaO, 24Na$_2$O, 6P$_2$O$_5$	Ciprofloxacin	N.A.	N.A.
Rivadeneira et al.	BG 45S5	Tetracycline	Bacterial cell growth inhibition,	4 staphylococci

(RIVADENEIRA et al., 2014) *In vitro*	nanoparticles/collagen composites [mol%] 45SiO$_2$, 24Na$_2$O, 24CaO, 6P$_2$O$_5$	hydrochloride (TCH)	antibacterial efficacy was similar for all TCH concentrations: 0.05, 0.20, 0.35 mg ml^{-1}	strains: S. *aureus* ATCC29213, ATCC25923, ATCC6538P and S. *epidermidis* ATCC12228.
Domingues et al. (DOMINGUES et al., 2004) *In vitro/ In vivo* **(animal model)**	BG [mol%] 80SiO$_2$, 16 CaO, 4P$_2$O$_5$	- Tetracycline hydrochloride (BT) -Complex formed by tetracycline and beta-cyclodextrin (BTC)	-A significant bacteriostatic activity was found with BT and BTC glasses. -Cyclodextrin slowed down the release of tetracycline for a long period of time. -Bactericidal activity increased when BG was loaded with tetracycline	A. *actinomycetemcomitans*
Rivadeneira et al.(RIVADENEIRA et al., 2015) *In vitro*	Agar–gelatin (AG) 45S5 BG microparticles composites [mol%] 45SiO$_2$, 24Na$_2$O, 24CaO, 6P$_2$O$_5$	Vancomycin hydrochloride (VC)	-Bacterial cell viability for *S. aureus* ATCC6538 was considerably inhibited after 24 and 48h of incubation. -AG-BG samples loaded with VC did not reduce the number of bacteria below 10^5 cfu (colony forming units) ml^{-1}	3 staphylococcus strains: S. *aureus* ATCC29213, S. *aureus* ATCC6538, and S. *epidermidis* ATCC12228.

Yao et al. (YAO et al., 2013) *In vitro*	45S5 BG scaffolds coated with polycaprolactone and vancomycin-loaded chitosan, [mol%] $45SiO_2, 24Na_2O, 24CaO, 6P_2O_5$	Vancomycin	N.A.	N.A.
Jia et al. (JIA et al., 2010) *In vitro/in vivo (osteomyelitis induced in an animal model)*	Borate BG and chitosan composite [mol.%] 6Na2O, 8K2O, 8MgO, 22CaO, 54B2O3, 2P2O5	Teicoplanin (TBGC)	*In vivo*: efficient therapeutic effect was revealed in animals implanted with TBGC pellets, showing an inferior positive rate of MRSA culture.	Methicillin-resistant S. *aureus* (MRSA)

* BG composition is not specified in the study. N.A.: not applied, study has not performed specific antibacterial tests

2.4 MULTIFACTORIAL ASPECTS INFLUENCING BIOACTIVE GLASS TO EMBED BIOFILM INHIBITORS

Biofilms in infected implanted tissues have an unquestionable clinical significance; for that reason, clinical guidelines involving effective protocols and superior biomaterials must be established for infection management. It is remarkable that the majority of studies dealing with antibacterial materials does not mention or consider in detail antibacterial activity. In general, studies show proper antibacterial activity against planktonic bacteria. Those studies suggest that a "proper" antibacterial activity is necessary for should be considered for future medical applications in bone infection therapy [4, 56]. However, it can be considered a controversial issue if the antibacterial effect achieved in those studies is sufficiently effective to treat human infections [57]. Other previous studies have evaluated anti-biofilm activity against mono-species biofilm formation [29, 58]. Perez-Tanoira et al. for example, reported that S53P4 BG prevented bacterial and biofilm adhesion, however this study; nevertheless, this study tested solely staphylococcal biofilm inhibition. Other recent studies have tested anti-biofilm properties of compounds against multi-species biofilms. Bortolin et al [59] revealed that S53P4 BG was able to reduce biofilm composed of S. *epidermis*, *A. baumanii,* and K. *pneumoniae*. Furthermore, Drago et al. [60] reported that S53P4 BG revealed a relevant biofilm inhibition effect on S. *aureus* and P. *aureginosa*. In principle, even if studies that analyze antibiofilm effects are reliable; increased efforts involving in *vivo* studies are needed to simulate realistic human infection conditions.

Human body infections, especially bone infections, are complex, and cannot be controlled by antibacterial effects solely. In general, bone infections are hard to treat due to diverse biological factors, notably vascular insufficiency, where systemic antibiotics and host immune cells are not able to reach the infected area through the blood stream.16 In addition, bone infections induced by multi-species biofilm formation increase antibiotic resistance and bacteria pathogenicity.12,15 Accordingly, bone infection treatment should focus primarily on inhibiting biofilm formation [61]. Nowadays, there are limited effective therapies specifically targeting biofilm formation. Mechanical debridement for infected bone removal is the most accepted clinical procedure [16]. Therefore, if bone debridement could be complemented by the application of an efficient anti-biofilm agent, for example based

on mesoporous bioactive glasses as discussed in this review, such biomaterial will be a promising candidate for bone infection treatment, as schematically illustrated in Figure 1.
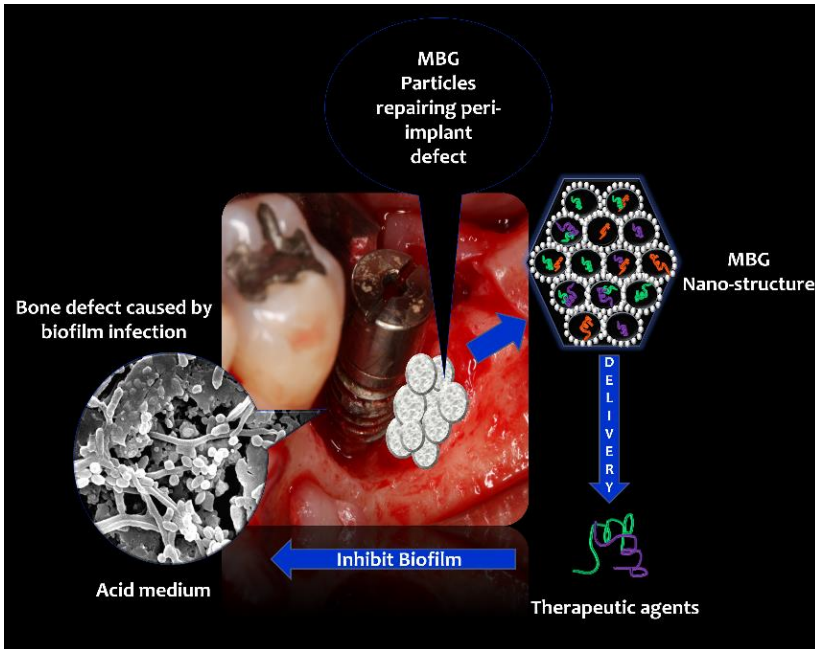
Figure 1. Schematic diagram showing mesoporous BG loaded with antibacterial agents applied and delivered at infected implanted receptor sites with an acid medium to inhibit biofilm proliferation and repair bone defects.

Another factor to consider is the type of active compound embedded into the BG carrier. As mentioned above, studies have been performed involving natural organic compounds such as essential oils and phototherapeutics as essential oils, which appear as valid alternatives for synthetic drugs [34, 36]. Consequently, new challenges have emerged to incorporate natural derived agents into BG compositions with the purpose of inducing antibacterial and health-promoting effects at receptor sites. Additionally, MBGs with highly organized structure have been reported to favor angiogenic and osteogenic responses [17, 20, 62]. For this reason, promising future approaches should consider MBG advantages and develop mechanisms to encapsulate pharmacological agents based on phytotherapeutics into wellorganized MBGs to enhance bone repair, inhibit biofilm formation, and reduce toxic effects. Indeed understanding the synergetic effects of

the release of both therapeutic ions and organic antibacterial agents remains a subject of high interest for future studies.

In this context, identifying parameters that influence the performance of MBGs as drug carriers is crucial to improve their action in infected receptor areas. Bone receptor surgical sites are inflammatory acidic areas where local acidosis increases due to the presence of bacterial metabolism byproducts like fatty acids and lactic acid produced infiltrated neutrophils [63]. MBG based drug delivery systems could take advantage of this acidic condition when applied on infected receptor areas and become a pH sensitive drug delivery structure, as schematically shown in Figure 13, [64]. Previous studies have shown that gentamicin released from MBG is pH dependent. Xia et al.64 reported MBGs as dual drug delivery systems where individual drugs could be released at different rates depending on the pH values of the surrounding area. Also, another study [65] established that gentamicin-loaded MBG exhibited drug release sensitive to the pH and the ionic composition of the surrounding medium. Consequently, significant features from receptor implanted sites such as biofilm accumulation and infiltrated inflammatory cells should be considered in forthcoming studies to enhance the capabilities of BGs as controlled delivery systems for anti-infective agents that can possess continuous action and efficient release.

2.5 CONCLUSIONS AND OUTLOOK

The majority of the reviewed scientific literature in the field of antibacterial materials has focused on in vitro and in vivo assays in specific models. Furthermore, most of the studies assessed antibacterial efficiency in planktonic bacteria cultures, which do not mimic a genuine infected tissue environment. Underestimation of biofilm significance in bone infection and repair procedures is a matter of concern, since studies may represent unrealistic conditions and they could be assessing antibacterial agents that may be inefficient or do not have the desired effects in future clinical applications. In fact, diverse multifactorial features influence the bioactive glass capability of being simultaneously an antibacterial, antibiofilm, and repairing biomaterial. Such factors involve incorporation of different biocompatible organic compounds with antibacterial and anti-biofilm potential, evaluation of receptor site conditions, drug delivery efficiency, and understanding synergetic effects with the intrinsic metallic ion release capability of BGs in the context of osteogenic and angiogenic response. The mentioned

characteristics can improve BGs making them biomaterials of choice for bone infection treatment and bone repair applications. In this context, further comprehensive in vitro and in vivo studies applying mesoporous bioactive glass incorporating effective anti-biofilm compounds at infected receptor sites are required.

2.6 REFERENCES

1. Quarto R, Giannoni P. Bone tissue engineering: Past-presentfuture. Methods Mol Biol 2016;1416:21–33. doi:10.1007/978-1-4939-3584-0_2.

2. Rezwan K, Chen QZ, Blaker JJ, Boccaccini AR. Biodegradable and bioactive porous polymer/inorganic composite scaffolds for bone tissue engineering. Biomaterials 2006;27:3413–3431. () doi: 10.1016/j.biomaterials.2006.01.039.

3. Hench LL. Opening paper 2015- Some comments on Bioglass: Four eras of discovery and development. Biomed Glas 2015;1:1–11. doi:10.1515/bglass-2015-0001.

4. Gubler M, Brunner TJ, Zehnder M, Waltimo T, Sener B, Stark WJ. Do bioactive glasses convey a disinfecting mechanism beyond a mere increase in pH? Int Endod J 2008;41:670–678. doi:10.1111/j.1365-2591.2008.01413.x.

5. Zhang D, Munukka E, Lepparanta O, Hupa L, Yl € anen H, Salonen J, € Eerola E, Viljanen MK, Hupa M. Comparison of antibacterial effect of three bioactive glasses. Key Eng Mater 2006;309–311 I:345–348.http://www.scopus.com/inward/record.url?eid52-s2.0-33645385660&partnerID540&md5547b7f40cb62189e0d04ad758cffafe55.

6. Hu S, Chang J, Liu M, Ning C. Study on antibacterial effect of 45S5 Bioglass. J Mater Sci Mater Med 2009;20:281–286. doi: 10.1007/s10856-008-3564-5.

7. Cui X, Gu Y, Li L, Wang H, Xie Z, Luo S, Zhou N, Huang W, Rahaman MN. In vitro bioactivity, cytocompatibility, and antibiotic release profile of gentamicin sulfate-loaded borate bioactive glass/chitosan composites. J Mater Sci Mater Med 2013;24:2391– 2403. doi:10.1007/s10856-013-4996-0.

8.   Salehi S, Davis HB, Ferracane JL, Mitchell JC. Sol-gel-derived bioactive glasses demonstrate antimicrobial effects on common oral bacteria. Am J Dent 2015;28:111–115. http://www.scopus.com/ inward/record.url?eid52-s2.0-84930736821&partnerID5tZOtx3y1.

9.   Stoor P, Soderling E, Grenman R. Interactions between the bioactive glass S53P4 and the atrophic rhinitis-associated microorganism klebsiella ozaenae. J Biomed Mater Res 1999;48:869–874.

10. Mehrvarzfar P, Akhavan H, Rastgarian H, Akhlagi NM, Soleymanpour R, Ahmadi A. An in vitro comparative study on the antimicrobial effects of bioglass 45S5 vs. calcium hydroxide on Enterococcus faecalis. Iran Endod J 2011;6:29–33. http://www.scopus.com/inward/record.url?eid52-s2.0-80051518645&partnerID5tZOtx3y1.

11. Rahaman MN, Bal BS, Huang W. Review: Emerging developments in the use of bioactive glasses for treating infected prosthetic joints. Mater Sci Eng C Mater Biol Appl 2014;41:224–231. doi:10.1016/j.msec.2014.04.055.

12. Davies D. Understanding biofilm resistance to antibacterial agents. Nat Rev Drug Discov 2003;2:114–122. doi:10.1038/nrd1008.

13. Olson ME, Ceri H, Morck DW, Buret AG, Read RR. Biofilm bacteria: Formation and comparative susceptibility to antibiotics. Can J Vet Res 2002;66:86–92.

14. Dongari-Bagtzoglou A. Pathogenesis of mucosal biofilm infections: Challenges and progress. Expert Rev Anti Infect Ther 2008; 6:201–208. doi:10.1586/14787210.6.2.201.

15. Davey ME, O'toole GA. Microbial biofilms: From ecology to molecular genetics. Microbiol Mol Biol Rev 2000;64:847–867. doi: 10.1128/MMBR.64.4.847-867.2000.

16. Brady RA, Leid JG, Calhoun JH, Costerton JW, Shirtliff ME. Osteomyelitis and the role of biofilms in chronic infection. FEMS Immunol Med Microbiol 2008;52:13–22. doi:10.1111/j.1574-695X.2007.00357.x.

17. Hum J, Boccaccini AR. Bioactive glasses as carriers for bioactive molecules and therapeutic drugs: A review. J Mater Sci Mater Med 2012;23:2317–2333. doi:10.1007/s10856-012-4580-z.

18. Sanchez-Salcedo S, Shruti S, Salinas AJ, Malavasi G, Menabue L, Vallet-Regı M. In vitro antibacterial capacity and cytocompatibility of SiO 2-CaO-P2O5 meso-macroporous glass scaffolds enriched with ZnO. J Mater Chem B 2014;2:4836–4847. doi:10.1039/c4tb00403e.

19. Wu C, Chang J. Mesoporous bioactive glasses: Structure characteristics, drug/growth factor delivery and bone regeneration application. Interface Focus 2012;2:292–306. doi:10.1098/rsfs.2011.0121.

20. Vallet-Regı M, Ruiz-Hernandez E. Bioceramics: From bone regeneration to cancer nanomedicine. Adv Mater 2011;23:5177–5218. doi:10.1002/adma.201101586.

21. Goh YF, Alshemary AZ, Akram M, Kadir MRA, Hussain R. Bioactive glass: An in-vitro comparative study of doping with nanoscale copper and silver particles. Int J Appl Glas Sci 2014;5:255– 266. doi:10.1111/ijag.12061.

22. Bellantone M, Williams HD, Hench LL. Broad-spectrum bactericidal activity of Ag2O-doped bioactive glass. Antimicrob Agents Chemother 2002;46:1940–1945. doi:10.1128/AAC.46.6.1940-1945.2002.

23. Coleman NJ. Aspects of the in vitro bioactivity and antimicrobial properties of Ag1- and Zn21-exchanged 11 A... tobermorites. J Mater Sci Med 2009;20:1347–1355. doi:10.1007/s10856-009-3698-0.

24. Hoppe A, Guldal NS, Boccaccini AR. A review of the biological € response to ionic dissolution products from bioactive glasses and glass-ceramics. Biomaterials 2011;32:2757–2774. doi:10.1016/j.biomaterials.2011.01.004.

25. Lindfors NC. Bioactive glass S53P4 as a bone graft substitute in the treatment of osteomyelitis. Bioact Glas Mater Prop Appl 2011; 47:209–216. doi:10.1016/B978-1-84569-768-6.50009-0.

26. Waltimo T, Brunner TJ, Vollenweider M, Stark WJ, Zehnder M. Antimicrobial effect of nanometric bioactive glass 45S5. J Dent Res 2007;86:754–757.

27. Allan I, Newman H, Wilson M. Particulate bioglass reduces the viability of bacterial biofilms formed on its surface in an in vitro model. Clin Oral Implants Res 2002;13:53–58.

28. Rathke A, Staude R, Muche R, Haller B. Antibacterial activity of a triclosan-containing resin composite matrix against three common oral bacteria. J Mater Sci Mater Med 2010;21:2971–2977. doi: 10.1007/s10856-010-4126-1.

29. Xu YT, Wu Q, Chen YM, Smales RJ, Shi SY, Wang MT. Antimicrobial effects of a bioactive glass combined with fluoride or triclosan on Streptococcus mutans biofilm. Arch Oral Biol 2015;60: 1059–1065. doi:10.1016/j.archoralbio.2015.03.007.

30. Bedoux G, Roig B, Thomas O, Dupont V, Le Bot B. Occurrence and toxicity of antimicrobial triclosan and by-products in the environment. Environ Sci Pollut Res Int 2012;19:1044–1065. doi: 10.1007/s11356-011-0632-z.

31. Dann AB, Hontela A. Triclosan: Environmental exposure, toxicity and mechanisms of action. J Appl Toxicol 2011;31:285–311. doi: 10.1002/jat.1660.

32. Salles Branco-de-Almeida L, Mendonca Murata R, Melo Franco E, Dos Santo M, De Alencar S, Koo H, Rosalen P. Effects of 7-Epiclusianone on Streptococcus mutans and caries development in rats. Planta Med 2011;77:40–45. doi:10.1055/s-0030-1250121.

33. Bakkali F, Averbeck S, Averbeck D, Idaomar M. Biological effects of essential oils—A review. Food Chem Toxicol 2008;46:446–475. doi:10.1016/j.fct.2007.09.106.

34. Prabhu M, Ruby Priscilla S, Kavitha K, Manivasakan P, Rajendran V, Kulandaivelu P. In vitro bioactivity and antimicrobial tuning of bioactive glass nanoparticles added with neem (Azadirachta indica) leaf powder. Biomed Res Int 2014;2014:950691–950610. doi: 1155/2014/950691.

35. Subapriya R, Nagini S. Medicinal properties of neem leaves: A review. Curr Med Chem Anticancer Agents 2005;5:149–146. doi: 10.2174/1568011053174828.

36. Bonfim RA, Chitarra VR, Gomes RT, Zacarias RD, Santos VR, Vasconcelos WA. Antimicrobial activity of bioactive glass associated to Brazilian red and green propolis. Planta Med 2009;75: 1078. ://WOS:000268806600766.

37. Jafarzadeh Kashi T, Kasra Kermanshahi S, Erfan R, Vahid Dastjerdi M, Rezaei EY, Tabatabaei FS. Evaluating the in-vitro

antibacterial effect of Iranian propolis on oral microorganisms. Iran J Pharm Res 2011;10:363–368.

38. Liberio SA, Pereira ALA, Araujo MJAM, Dutra RP, Nascimento FRF, Monteiro-Neto V, Ribeiro MN, Goncalves AG, Guerra RNM. The potential use of propolis as a cariostatic agent and its actions on mutans group streptococci. J Ethnopharmacol 2009;125:1–9. doi:10.1016/j.jep.2009.04.047.

39. Mori GG, da Rodrigues SS, Shibayama ST, Pomini M, do Amaral COF. Biocompatibility of a calcium hydroxide-propolis experimental paste in rat subcutaneous tissue. Braz Dent J 2014;25:104–108. http://www.ncbi.nlm.nih.gov/pubmed/25140713 (accessed September 18, 2016).

40. Sforcin JM. Biological properties and therapeutic applications of propolis. Phytother Res 2016;30:894–905. doi:10.1002/ptr.5605.

41. Grenho L, Barros J, Ferreira C, Santos VR, Monteiro FJ, Ferraz MP, Cortes ME. In vitro antimicrobial activity and biocompatibility of propolis containing nanohydroxyapatite. Biomed Mater 2015; 10:25004. doi:10.1088/1748-6041/10/2/025004.

42. Wu C, Chang J. Multifunctional mesoporous bioactive glasses for effective delivery of therapeutic ions and drug/growth factors. J Control Release 2014;193:282–295. doi:10.1016/j.jconrel.2014.04.026.

43. Mourino V, Boccaccini AR. Bone tissue engineering therapeutics: Controlled drug delivery in three-dimensional scaffolds. JR Soc Interface 2010;7:209–227. doi:10.1098/rsif.2009.0379.

44. Li Y, Liu YZ, Long T, Yu XB, Tang TT, Dai KR, Tian B, Guo YP, Zhu ZA. Mesoporous bioactive glass as a drug delivery system: Fabrication, bactericidal properties and biocompatibility. J Mater Sci Mater Med 2013;24:1951–1961., doi:10.1007/s10856-013-4960-z.

45. Vallet-Regi M, Izquierdo-Barba I, Colilla M. Structure and functionalization of mesoporous bioceramics for bone tissue regeneration and local drug delivery. Philos Trans R Soc A Math Phys Eng Sci 2012;370:1400–1421. doi:10.1098/rsta.2011.0258.

46. Xie Z, Liu X, Jia W, Zhang C, Huang W, Wang J. Treatment of osteomyelitis and repair of bone defect by degradable bioactive

borate glass releasing vancomycin. J Control Release 2009;139: 118–126. doi:10.1016/j.jconrel.2009.06.012.

47. Nandi SK, Kundu B, Mukherjee P, Mandal TK, Datta S, De DK, Basu D. In vitro and in vivo release of cefuroxime axetil from bioactive glass as an implantable delivery system in experimental osteomyelitis. Ceram. Int 2009;35:3207–3216., doi:10.1016/j.ceramint.2009.05.005.

48. Miola M, Vitale-Brovarone C, Mattu C, Verne E. Antibiotic loading on bioactive glasses and glass-ceramics: an approach to surface modification. J Biomater Appl 2013;28:308–319. doi:10.1177/ 0885328212447665.

49. Mabrouk M, Mostafa AA, Oudadesse H, Mahmoud AA, El-Gohary MI. Effect of ciprofloxacin incorporation in PVA and PVA bioactive glass composite scaffolds. Ceram. Int 2014;40:4833–4845. doi: 10.1016/j.ceramint.2013.09.033.

50. Rivadeneira J, Di Virgilio AL, Audisio MC, Boccaccini AR, Gorustovich AA. Evaluation of antibacterial and cytotoxic effects of nano-sized bioactive glass/collagen composites releasing tetracycline hydrochloride. J Appl Microbiol 2014;116:1438–1446. doi: 10.1111/jam.12476.

51. Domingues ZR, Cortes ME, Gomes TA, Diniz HF, Freitas CS, Gomes JB, Faria AMC, Sinisterra RD. Bioactive glass as a drug delivery system of tetracycline and tetracycline associated with beta-cyclodextrin. Biomaterials 2004;25:327–333.

52. Rivadeneira J, Di Virgilio AL, Audisio MC, Boccaccini AR, Gorustovich AA. Evaluation of the antibacterial effects of vancomycin hydrochloride released from agar-gelatin-bioactive glass composites. Biomed Mater 2015;10:15011. doi:10.1088/1748-6041/10/1/015011.

53. Yao QQ, Nooeaid P, Roether JA, Dong YN, Zhang QQ, Boccaccini AR. Bioglass (R)-based scaffolds incorporating polycaprolactone and chitosan coatings for controlled vancomycin delivery. Ceram Int 2013;39:7517–7522. doi:10.1016/j.ceramint.2013.03.002.

54. Jia WT, Zhang X, Luo SH, Liu X, Huang WH, Rahaman MN, Day DE, Zhang CQ, Xie ZP, Wang JQ. Novel borate glass/chitosan composite as a delivery vehicle for teicoplanin in the treatment of

chronic osteomyelitis. Acta Biomater 2010;6:812–819. doi:10.1016/ j.actbio.2009.09.011.

55. Rastegar Lari A, Bahrami Honar H, Alaghehbandan R. Pseudomonas infections in Tohid Burn Center, Iran. Burns 1998;24:637–641. doi:10.1016/S0305-4179(98)00090-4.

56. Zhang D, Lepparanta O, Munukka E, Ylanen H, Viljanen MK, Eerola E, Hupa M, Hupa L. Antibacterial effects and dissolution behavior of six bioactive glasses. J Biomed Mater Res A 2010;93: 475–483. doi:10.1002/jbm.a.32564.

57. Xie ZP, Zhang CQ, Yi CQ, Qiu JJ, Wang JQ, Zhou J. Failure of particulate bioglass to prevent experimental staphylococcal infection of open tibial fractures. J. Antimicrob. Chemother 2008; 62:1162–1163. doi:10.1093/jac/dkn336.

58. Coraca-Huber DC, Fille M, Hausdorfer J, Putzer D, Nogler M. Efficacy of antibacterial bioactive glass S53P4 against S. aureus biofilms grown on titanium discs in vitro. J Orthop Res 2014;32:175– 177. doi:10.1002/jor.22463.

59. Bortolin M, De Vecchi E, Romano CL, Toscano M, Mattina R, Drago L. Antibiofilm agents against MDR bacterial strains: Is bioactive glass BAG-S53P4 also effective? J Antimicrob Chemother 2015. doi:10.1093/jac/dkv327.

60. Drago L, Vassena C, Fenu S, De Vecchi E, Signori V, De Francesco R, Romano CL. In vitro antibiofilm activity of bioactive glass S53P4. Future Microbiol 2014;9:593–601. doi:10.2217/ fmb.14.20.

61. Xavier JG, Geremias TC, Montero JFD, Vahey BR, Benfatti CAM, Souza JCM, Magini RS, Pimenta AL. Lactam inhibiting Streptococcus mutans growth on titanium. Mater Sci Eng C 2016; 68:837–841. doi:10.1016/j.msec.2016.07.013.

62. Liu YZ, Li Y, Yu XB, Liu LN, Zhu ZA, Guo YP. Drug delivery property, bactericidal property and cytocompatibility of magnetic mesoporous bioactive glass. Mater Sci Eng C Mater Biol Appl 2014; 41:196–205. doi:10.1016/j.msec.2014.04.037.

63. Lardner A. The effects of extracellular pH on immune function. J Leukoc Biol 2001;69:522–530. http://www.jleukbio.org/content/ 69/4/522.full#sec-1.

64. Xia W, Chang J, Lin J, Zhu J. The pH-controlled dual-drug release from mesoporous bioactive glass/polypeptide graft copolymer nanomicelle composites. Eur J Pharm Biopharm 2008;69:546–552. doi:10.1016/j.ejpb.2007.11.018.

65. Xia W, Chang J. Well-ordered mesoporous bioactive glasses (MBG): A promising bioactive drug delivery system. J Control Release 2006;110:522–530. doi:10.1016/j.jconrel.2005.11.002.

3 ARTIGO 2 EM INGLÊS

O artigo a seguir foi publicado na revista científica ***Journal of Biomedical materials research: part A***. Fator de impacto: 3.263. Qualis: A1

Inhibition of multi-species oral biofilm by bromide doped bioactive glass

M.E. Galarraga-Vinueza1, B. Passoni1, C. A. M. Benfatti1, J. Mesquita-Guimarães2, B. Henriques1, R. S. Magini1, M.C. Fredel2, B. V. Meerbeek3, W. Teughels4, J. C. M. Souza1,2*

1Center for Education and Research on Dental Implants (CEPID), Post-Graduate Program in Dentistry (PPGO), Department of Dentistry (ODT), Federal University of Santa Catarina (UFSC), Florianópolis/SC, 88040-900, Brazil
2Ceramic and Composite Materials Research Group (CERMAT), Federal University of Santa Catarina, Florianópolis 88040-900, Brazil
3Dept. of Oral Health Sciences, BIOMAT, University Hospitals Leuven, Katholieke Universiteit Leuven, Kapucijnenvoer 33, Leuven B-3000, Belgium
4Dept. of Oral Health Sciences, University Hospitals Leuven, Katholieke Universiteit Leuven, Kapucijnenvoer 33, Leuven B-3000, Belgium

Abstract:

Bioactive glass is an attractive biomaterial that has shown excellent osteogenic and angiogenic effects for oral bone repairing procedures. However, anti-biofilm potential related to such biomaterial has not been completely validated, mainly against multi species biofilms involved in early tissue infections. The aim of the present study was to evaluate the anti-biofilm effect of 58S bioactive glass embedding calcium bromide compounds at different concentrations. Bioactive glass containing 0, 5, or 10wt% CaBr2 was synthesized by alkali sol-gel method and then characterized by physco-chemical and scanning electron microscopy (SEM). Then, samples were tested by microbiological assays using optical density, real time q-PCR, and SEM. Bioactive glass particles showed accurate chemical composition and an angular shape with a bimodal size distribution ranging from 0.6 to 110 µm. The mean particle size was around 29 µm. A significant anti-biofilm effect was recorded

for 5wt% CaBr2-doped bioactive glass against *S. mitis, V. parvula, P. gingivais, S. gordoni, A. viscosus*, and *F. nucleatum*. Such species are involved in the biofilm structure related to infections on hard and soft tissues in the oral cavity. The incorporation of calcium bromide into bioactive glass can be a strategy to enhance the anti-biofilm potential of bioactive glasses for bone healing and infection treatment.

Key words: Bioactive glass, anti-biofilm, bromide, sol-gel synthesis, bone infection, bone healing

3.1 INTRODUCTION

Bioactive glass (BG) is a promising biomaterial developed 40 years ago by the American scientist Larry Hench who produced the first BG of 45S5 composition with the purpose of repairing human bone defects and derived infections [1,2]. Previous studies have widely shown the outstanding properties on 45S5 BG, such as stimulation of osteogenic cell migration, vascularization, dissolution in bone tissue, and antibacterial effects induced by ion release [3]. In the 90s, a bioactive glass named 58S was developed via sol-gel method, in order to obtain an alternative compound with similar properties to those recorded for 45S5. Sepulveda et al. showed that melt-derived 45S5 BG powders exhibited lower dissolution rates for hydroxyapatite formation in comparison to those on 58S sol gel-glass powder [4]. Accordingly, hydroxyapatite is fundamental for bone healing and remodeling. Thus, the formation of a carbonated hydroxyl-apatite (CHA) layer establishes a bioactive interface between bone and BG surface, mimicking the mineral phase of bone, that also induces osteogenic cell proliferation, resulting in a desired biological match between BG particles and human tissues [1,5,6]. Nonetheless, proper bioactive response is only one of the purposes of a bioactive material. Bone infection occurs in the range of 1-2.5% being an issue of orthopedic and oral surgeries [5,7,8]. In fact, biofilms are responsible for more than 80% of human infections [9,10] which influence the clinical use of antibiotics after surgical procedures.

The antibacterial effect revealed by BG has been attributed to the ion release capability in increasing the pH of the surrounding medium that can affect planktonic bacteria growth [11]. Most of the studies report that the BG antibacterial effect against specific planktonic bacteria do not reflect realistic conditions of biofilm growth and pathogenicity at infected areas [12–16]. Biofilm is a well-organized microbial community embedded in an extracellular polymeric matrix

composed of polysaccharides, nucleic acids, proteins and water, that adheres to different surfaces

such as teeth, rehabilitation synthetic materials, bone, and soft tissues [17,18]. As a result of a complex well-organized structure, bacteria embedded in biofilm is 1000 times more resistant to antibiotic therapy compared to planktonic bacteria [9,12]. Additionally, studies have shown that biofilm formation may enhance virulence of certain pathogenic bacteria like *P. gingivais* [19], *S. mitis*, *F. nucleatum*, *A. viscosus*, *A. actinomycetemcomitans,* and *V. parvula* [20]. In an attempt in improving BG antibacterial and anti-biofilm activity, several studies have reported positive antibacterial properties achieved by bioactive glasses embedded with inorganic compounds containing silver, cerium, selenium, magnesium, zinc, or fluoride [14,15,21–24]. Bromine, a chemical element corresponding to the halogen group, has been poorly explored in tissue engineering applications. One study reports the application of 12-methacryloyloxydodecylpyridinium bromide (MDPB) monomer as an antibacterial agent embedded in resinous biomaterials. That previous study reported an effective antibacterial and anti-biofilm activity of MDPB against S. mutans species over a period of 60 s. That was attributed to the inhibition of an enzyme named lactate dehydrogenase activitywhich is responsible for the S. mutans metabolism [25].

Nevertheless, there are no studies reporting the incorporation of $CaBr_2$-based compounds in BG composition to enhance its antibacterial activity. Therefore, the aim of the present study was to produce a bioactive glass embedding calcium bromide as an innovative strategy to inhibit biofilm formation avoiding infections at bone and surrounding tissues. The null hypothesis of this study was that the presence of bromide does not affect the multi-species biofilm growth on 58S bioactive glass.

3.2 MATERIALS AND METHODS

The methodology applied in this study to synthesize and analyze 58S bioactive glass embedding $CaBr_2$ is represented in Figure 1. First, BG (58 wt% SiO_2, 33 wt% CaO, 9 wt% P_2O_5) powder was processed by sol-gel method following a previous study performed by the authors [26]. For that, tetraethyl orthosilicate (TEOS) (98%, Sigma Aldrich, USA), triethyl phosphate (TEP) (99.8%, Sigma Aldrich, USA) and calcium nitrate tetrahydrate ($Ca(NO_3)2 \cdot 4H_2O$) (Vetec, Brazil) were used as precursors of silicon, phosphorous and calcium oxide, respectively.

Nitric acid (HNO$_3$, 68%, Vetec, Brazil) was used to dissolve Ca(NO$_3$)$_2$·4H$_2$O and to adjust pH solution while ethyl alcohol (EtOH, P.A., Synth, Brazil) was used to dissolve TEOS and TEP. Molar ratio of SiO$_2$, P$_2$O$_5$ and CaO was calculated, concerning the BG58S proportion. TEOS and TEP were placed in a glass recipient containing EtOH under magnetic stirring at 25 ^{o}C for 10 min. Ca(NO$_3$)$_2$·4H$_2$O was dissolved in 2 M HNO$_3$ and then added to water at a molar ratio TEOS:H$_2$O of 1:4. For bromide doped BG58S samples, calcium bromide hydrate (CaBr$_2$.xH$_2$O, Sigma-Aldrich, USA) was added as bromide precursor to achieve 5 or 10 wt% CaBr2. Considering the stoichiometric relation of calcium bromide, calcium nitrate quantity was calculated to maintain the final amount of 33wt% CaO. The mixtures were added to the solution and stirred for 1 h. Solution was placed in a chamber at 70 °C for drying over a period of 24 h. Subsequently, the material was thermally treated at 600 °C and milled in planetarium ball mill (PM100, Retsch, Germany) at 400 rpm for 1 h, to obtain the bioactive glass powder. BG powders were deagglomerated in a mortar agate with acetone. Then, BG powders were sieved at 106 μm and pressed at 80 MPa to obtain small discs of 10 mm diameter and 1 mm thickness. Thermal treatment was performed at 1150ºC, by 10 ºC/min heating rate and 180 min of holding time.
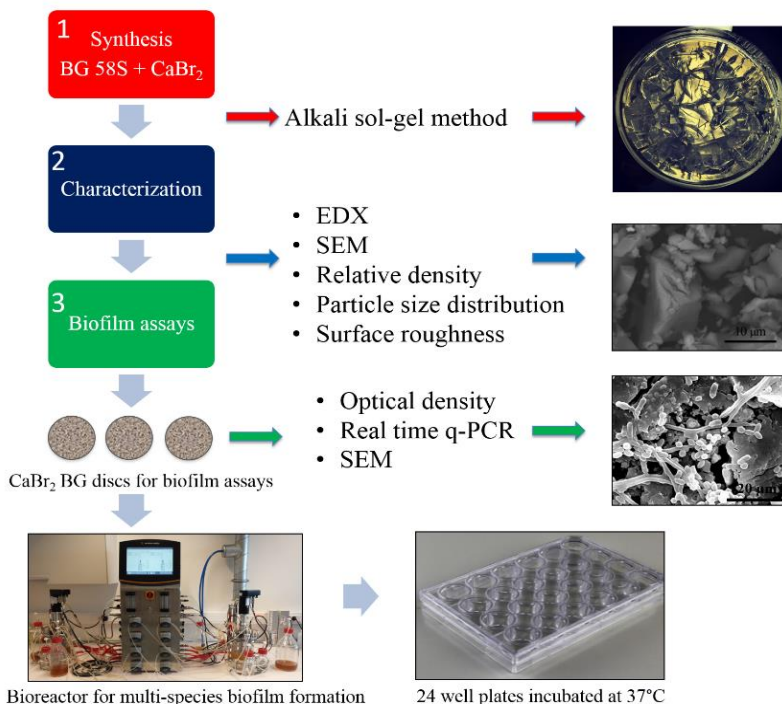
Figure 1. Schematic diagram showing the followed methodology to assess biofilm inhibition

Physico-chemical and morphological analyses

An initial chemical analysis was performed by energy dispersive X-ray spectroscopy (EDX, Swift 2000, Hitachi, Japan). The compound composition was obtained by rearranging the quantity of oxygen to calculate the weight percentage of oxides using the most stable stoichiometric arrangement, resulting in a reliable tool to semi-quantify the respective oxides. To evaluate the density of the sintered samples, the Archimedes Principle was applied to measure the relative density of the discs in green and after thermal treatment at 1150 ºC. The particle size distribution was measured in a laser diffraction equipment (Mastersizer 2000, Malvern, UK). The powder was introduced in a wet dispersion unit with low water rotation around 1200 rpm to avoid any deagglomeration of the sample. Before microbiological assays, the morphologic aspects of the BG particles as well as the surfaces of the test samples were analyzed by scanning electron microscopy (SEM),

(TM3030, Hitachi, Japan) at 15 kV by back-scattering electron (BSE) mode. Samples were sputter-coated with gold prior to SEM analysis. The roughness values of the disc samples were obtained regarding Rt (maximum height between peak and valley) and Ra roughness parameter that consists in the arithmetic mean value between the peak and valley height values in the effective roughness profile. The Ra roughness was recorded at five different areas on each material (n=25) using an optical profilometer (Zygo, NewView, 7300, USA). The measurement length was 0.7 mm and cut off at 0.25 mm for 3 s. Afterwards, a color map and 3D model representation of the surface roughness was performed per each sample using the Mountain map Software (Digital Surf, France). The X-ray diffraction (XRD) analysis was performed on the powder and thermal treated samples to evaluate the presence of crystalline phases in the amorphous matrix of the bioactive glass. The samples were analyzed in a diffractometer (D8 Discover, Bruker, Germany) by using Cu Kα radiation ($\lambda = 1.5406$ Å) on theta-2 theta mode. The range of analyzed angles was at 10-70º, with a step size of 0.04º and 1 s of step time. The peaks for each phase were identified using X'Pert High Score Plus Software (Panalytical, USA) within JCPDS patterns database.

Biofilm growth conditions

Bioglass discs with different concentrations of $CaBr_2$ (0%, 5% or 10%), were tested against a multi-species biofilm, grown in a bioreactor (BIOSTAT® B, Germany) simulating the oral conditions as illustrated Figure 1. The multi-species form included 10 strains as follow: 2 early colonizer bacterial species (*Streptococcus mitis* and *Streptococcus gordonii*), 5 pathogen bacterial species (*Fusobacterium nucleatum*, *Porphyromonas gingivalis*, *Prevotella intermedia*, *Streptococcus mutans, Streptococcus sobrinus*) and 3 beneficial bacterial species (*Veillonella parvula, Actinomyces viscosus, Streptococcus salivarius*). 750ml of BHI II [27] 37 g/L containing brain heart infusion broth, 2.5 g/L mucin from porcine stomach type III (Sigma-Aldrich Chemie GmbH, Buchs, Switzerland), 1g/L yeast extract, 0.1 g/L L-cysteine, 2 g/L sodium bicarbonate was added to the bioreactor vessel. Also, the calibration of pH electrode was performed with 1/10 HCl 1/10 and the 1 molar NaOCl before the sterilization process. Yet, one vessel of 2L was prepared with fresh BHI II, in order to be able to refresh the growth medium twice a day, over the experiment period. After the sterilization process, the bioreactor was set-up with 300 rpm of stirring on anaerobic

condition at 37°C. Also, an anti-foam liquid was added before the overnight wait.

Bacterial strains were grown overnight at 37°C in BHI under aerobic or anaerobic conditions, as described in the ATCC recommendations for each strain and then incubated in the bioreactor. After 24 h, the bioreactor medium was supplemented with 5 mg/L hemin, 1 mg/L menadione, and the absorbance of medium was adjusted to zero. After this procedure, the absorbance of the bacterial suspension was controlled to achieve the same optical density values prior to incubation in the bioreactor. Stable multi-species biofilm were obtained for 72 h. After this period, BG discs were placed at the bottom of 24 well-plates. Each well containing a BG disc was filled-up with 900 μL fresh BHI and 100 μL bioreactor culture. The negative and positive control groups had pure bioglass discs. However, the negative control group received 900 µL fresh BHI and 100 µL bioreactor culture while the positive control group was tested with 400 μL chlorhexidine, 500 μL fresh BHI and 100 bioreactor culture. The 24 well plates were incubated at 37°C under anaerobic conditions over a period of 24 h biofilm growth. Then, the supernatant was carefully removed with pipets, and therefore the discs were smoothly cleaned two times with 300 μL PBS to withdrawn the weakly attached biofilm. The well-attached biofilm was removed with 300 µL trypsin, into an anaerobic jar and maintained into the incubator for 15 min. The trypsin from each well was added to Eppendorf's to be centrifuged and then the pellets were resuspended in 500 μL PBS. On such dilution, a vitality DNA extraction was performed using 10 μL PMA and 90 μL bacterial dilution in PBS. The real time q-PCR was performed in triplicate for each strain using the ABI 7700 Sequence Detection System platform (Applied Biosystems, Foster City, CA, USA) [28]. Data was exported to an excel sheet to analyze the amount of each strain into the biofilm. For microscopic analyses, discs covered with biofilms were washed two times in PBS and fixed in glutaraldehyde 2% for 5 min. Then, discs were washed three times in PBS, and dehydrated through a series of graded ethanol solutions (50, 70, 80, 90, 100%). Samples covered with biofilms were sputter-coated with gold, and analyzed by scanning electron microscopy.

3.3 RESULTS

The particle size distribution of BG58S particles revealed a bimodal distribution with particle size ranging from 0.6 up to 110 µm,

as seen in Figure 2. The mean particle size was around 29 μm. The chemical composition of 58S MBG powder particles was quite similar to the expected composition (58.2 ± 2 wt% SiO2, 33.01 ± 1 wt% CaO, 9 ± 1 wt% P2O5), as detected by EDX analyses. The EDX spectra of all compositions are shown in Figure 3. The EDX spectra showed the highest intensity peak for Si element. The intensity of Ca element is intermediary while the peak for P element was the lowest in the spectra. Furthermore, the bioactive glasses embedding CaBr2 revealed an increase in the Br peak with the increase of CaBr2 in the composition.
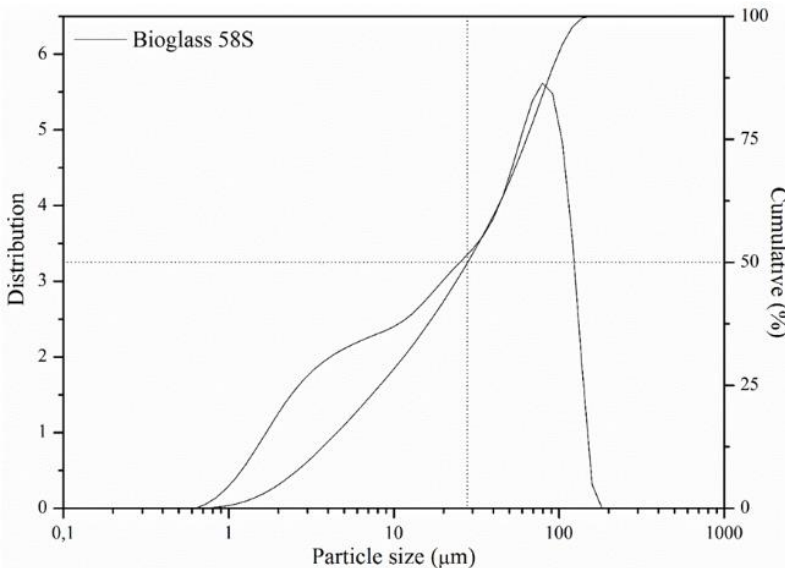
Figura 2. 58S BG Bimodal particle size distribution

XRD spectra for the powders and heat pressed 58S bioactive glass samples free of $CaBr_2$ are shown in Figure 4 while XRD spectra for samples embedding $CaBr_2$ are shown in Figures 5 and 6. The XRD spectra of the bioactive glass powders revealed a broad diffraction band, confirming its amorphous and glassy nature [4,31,32]. Moreover, peaks of tetracalcium phosphate (TTCP), dicalcium silicate (DCS) and bromine oxide were identified that confirmed the success of the modified sol-gel synthesis. The increase of bromine phases was noticed with increasing of the amount of CaBr2 in the bioactive glass composition. Considering the crystalline phases, XRD peaks for calcium phosphate phases, wollastonite, pseudowollastonite and quartz were detected as tresult from the high heat treatment [32–36].

Pseudowollastonite is a polymorph of wollastonite, that possesses a transition temperature around 1250 ºC. However, the excess of SiO2 favors the formation of the pseudowollastonite at lower temperatures [35,36]. In the case of the XRD spectra for BG58S 5%CaBr$_2$, the crystalline phases of quartz, tricalcium phosphate, wollastonite and phosphorus bromide were detected after 1150 ºC. The increase in the crystallization intensity of quartz can be explained by the decomposition of dicalcium silicate, in CaO and SiO$_2$ [35,36]. Phosphorus bromide crystallizes from the decomposition of tetracalcium phosphate into β-tricalcium phosphate, releasing phosphates to react with bromine oxide [35, 36]. In the case of the XRD spectra recorded for BG58S CaBr$_2$ 10wt%, calcium phosphate silicate, pseudowollastonite, wollastonite and silicon bromide phases were detected after thermal treatment at 1150 ºC. That indicated that the silicon was not available to crystallize alone and therefore it reacted almost on totality with the bromine oxide to crystallize silicon bromide. That can be associated with the excess of CaBr$_2$ in such chemical composition. However, the thermal treatment promoted the formation of pseudowollastonite and wollastonite [32, 35, 36].
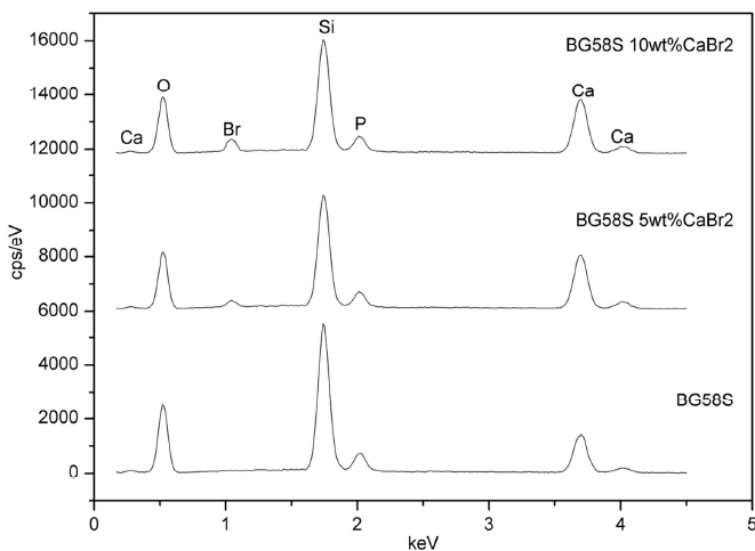
Figura 3. EDX spectra recorded for 58S bioactive glass free of CaBr$_2$ and including 5 or 10% CaBr$_2$
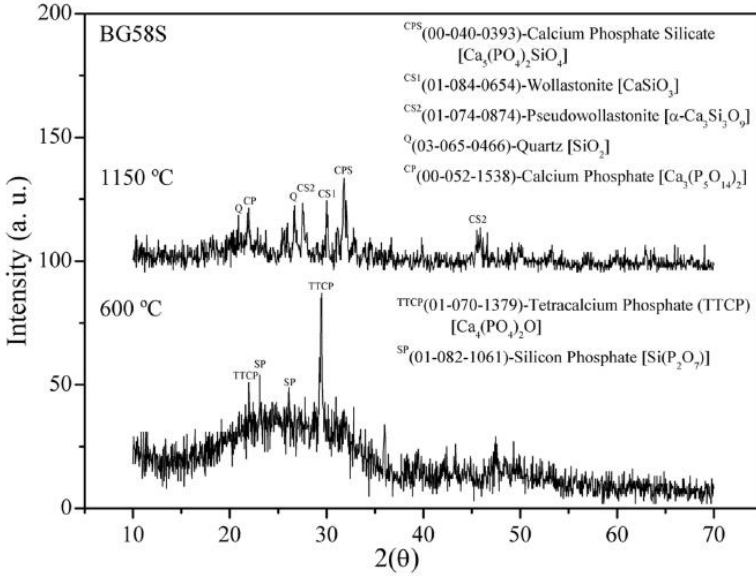
Figure 4. XRD spectra recorded for 58S bioactive glass samples free of $CaBr_2$ processed at 600 or 1150 ^oC.
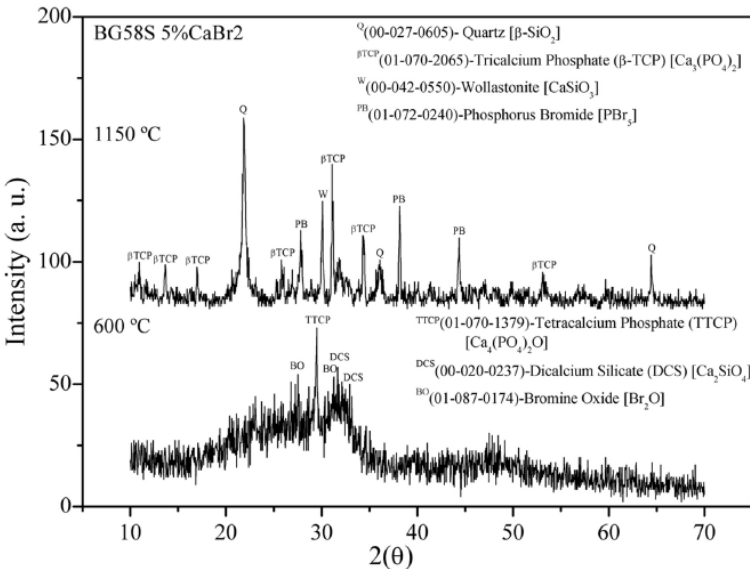
Figure 5. XRD spectra recorded for 58S bioactive glass samples embedding 5% CaBr2 processed at 600 or 1150 ^oC
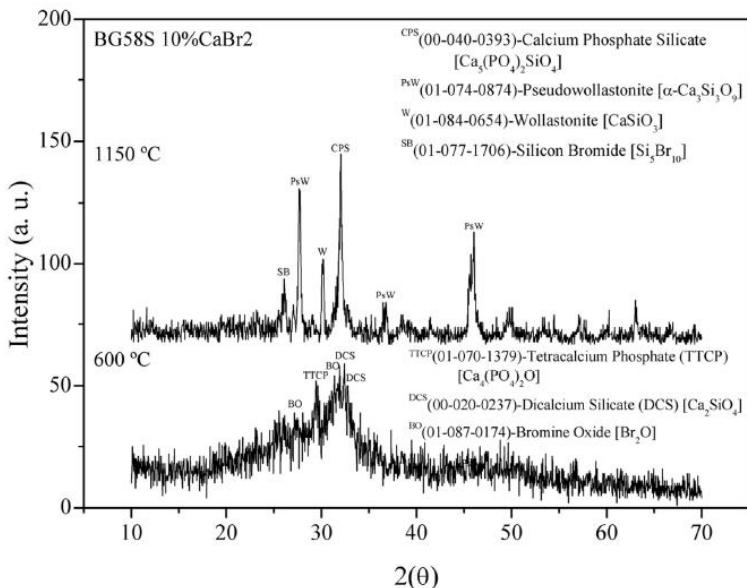
Figure 6. XRD spectra recorded for 58S bioactive glass samples embedding 10% CaBr$_2$ processed at 600 or 1150 ^{o}C

SEM images revealed 58S bioactive glass powder having an angular shape morphology that is typical from glass milling procedure (figure 7). BG58S samples containing CaBr$_2$ 5wt% before thermal treatment revealed needle like crystals typical from calcium phosphate phases [29]. Such crystals disappeared and formed angular lighter crystals like β-Tricalcium phosphate after thermal treatment at 1150 ºC [30]. Surfaces of bromide-doped 58S BG discs revealed a rough morphologic aspect associated with the content of CaBr$_2$ as shown in figure 7. Thus, the presence of CaBr$_2$ seemed to affect the densification process of the bioactive glass. Thermal treatment performed at a higher temperature and longer holding time should promote an increase in atomic diffusion rates, leading to the formation of larger and structural ordered particles.
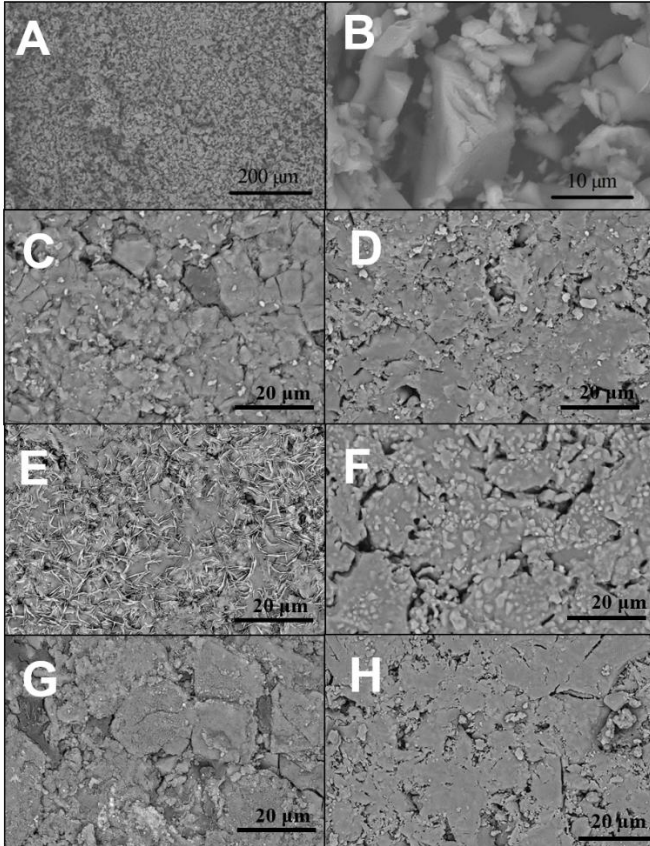
Figure 7. SEM images of BG 58S 5wt % CaBr$_2$ powder (A and B), 58S BG discs before (C, E and G) and after (D, F and H) thermal treatment incorporating 0, 5, and 10 wt % CaBr$_2$ correspondingly

The arithmetic average roughness (Ra) values and maximum height between peak and valley values (Rt) recorded on 58S BG discs increased with CaBr$_2$ content as shown and illustrated in Figure 8. The relative density of the samples were determined via Archimedes method before and after thermal treatment. Several thermal cycles were assessed at maximum temperature ranging from 600 up to 1250 oC in order to achieve a high density for the samples. A proper maximum temperature at 1150 ºC of thermal treatment was selected considering final shape and high density for microbiological assays. The relative density of the samples before the thermal treatment was higher than 50%.

Additionally, the relative density of those samples increased with the $CaBr_2$ content. In a similar way, the sintered samples had a relative density of more than 74%, which increased directly with the $CaBr_2$ content, achieving around 95% relative density on the highest concentration of $CaBr_2$ (Figure 9).
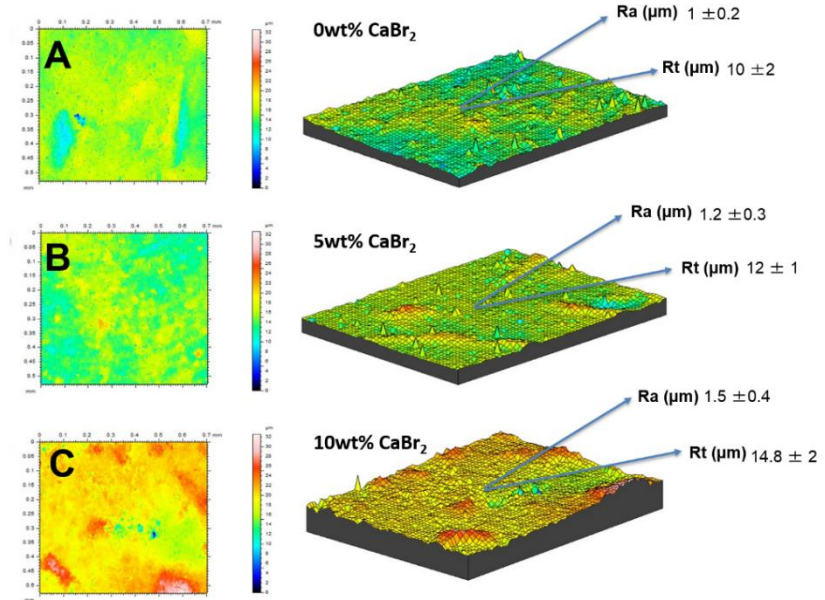
Figure 8. Ra, Rt roughness values, color map and 3D representation of surface roughness for 0, 5, and 10wt% $CaBr_2$ doped 58S BG discs after thermal treatment up to $1150^{o}C$
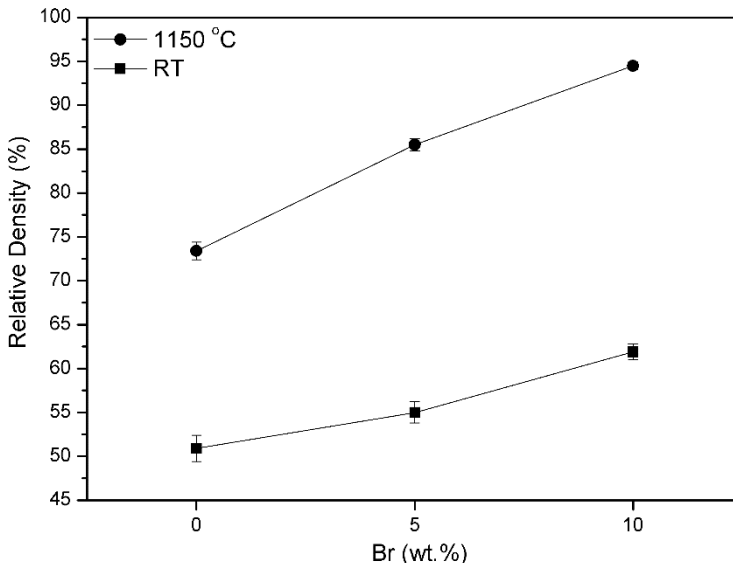
Figure 9. Relative densities of green and sintered discs of BG 58S containing or not 5wt% or 10wt% CaBr$_2$

Biofilm Inhibition

A significant biofilm inhibition, represented by the decrease of bacterial cell amount, was noticed when the chlorhexidine was placed in contact with the multi-species biofilm grown on the 58SBG discs free of CaBr$_2$. That validated the antimicrobial effect of chlorhexidine against all the early, beneficial and pathogenic species tested in this study. The amount of bacteria also decreased in the presence of 58SBG discs doped with 5% CaBr$_2$ regarding *S. mitis* and *S. gordonii* (early colonizers*), V. parvula* and *A. viscosus* (beneficial species), and *P. gingivalis* (pathogenic species). However, no decrease of bacterial amount was detected for multi-species biofilm grown on 58S BG discs doped with 10wt% CaBr$_2$. Results of biofilm inhibition obtained by q-PCR analyses for early, beneficial, and pathogen bacteria are shown in Figures 10 and 11. SEM inspection of the 58S BG discs surfaces covered with multi-species biofilms is shown in Figure 12. Considering the morphology of the multi-species biofilm tested in the present study, streptococcus, bacillus, and filamentous species can be detected on bioactive glass surfaces free or containing CaBr$_2$ after 24h of multi-species biofilm growth (Fig. 12). The multi-species biofilm revealed similar morphological aspects on all the test samples inspected by SEM.
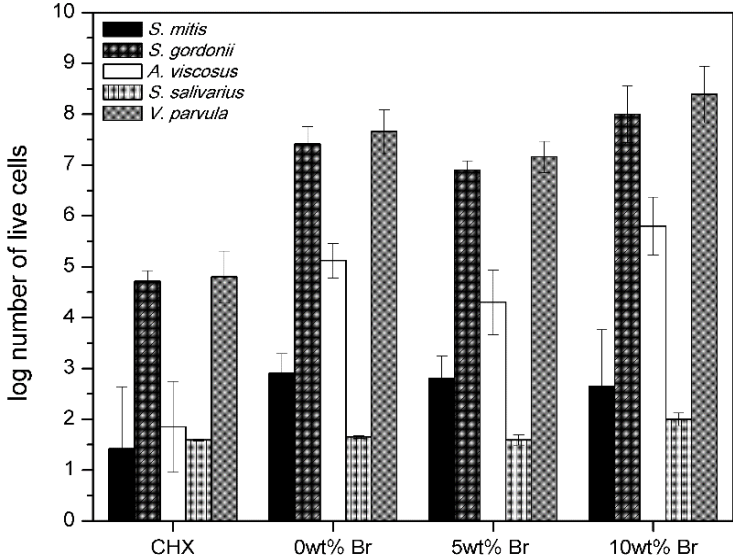
Figure 10. . Inhibition of early and beneficial oral biofilm species on 0wt% CaBr$_2$ 58S BG discs with chlorhexidine (CHX) (positive control group), 0wt% CaBr$_2$ BG58S discs (negative control group), 5 or 10 wt% CaBr$_2$ BG58S discs
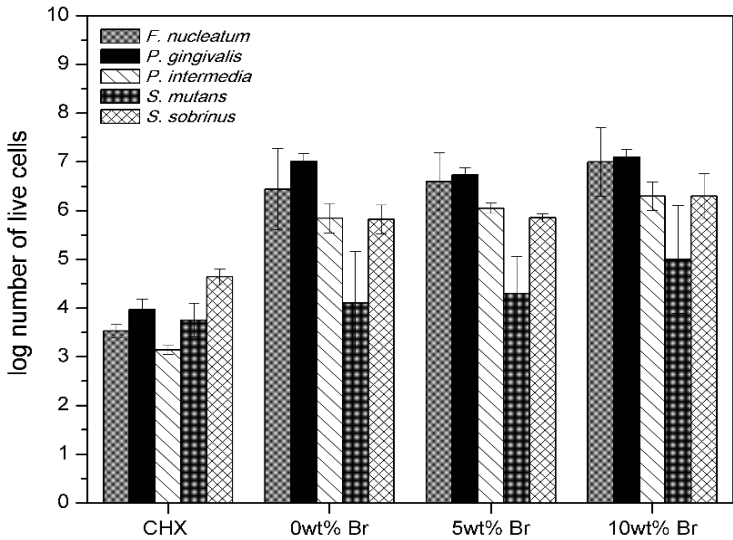
Figure 11. Inhibition of pathogen oral biofilm species on 0wt% CaBr$_2$ BG58S discs with chlorhexidine (CHX) (positive control group), 0wt% CaBr$_2$ BG58S discs (negative control group), and 5, 10 wt% CaBr$_2$ BG58S discs
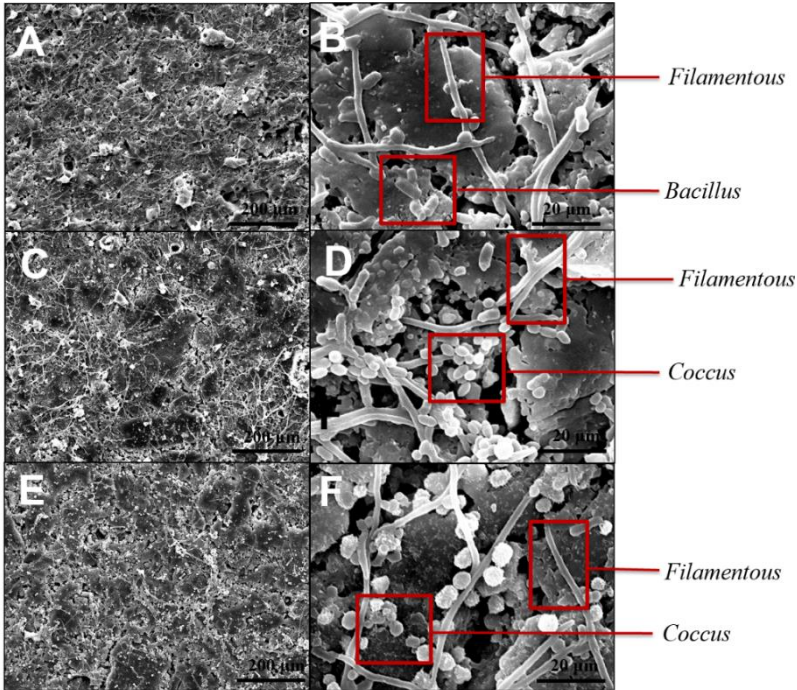
Figure 12. SEM images of multi-species biofilm adherence on BG58S discs with 0wt%CaBr$_2$ (A,B), 5wt% CaBr$_2$(C,D) and 10 wt% CaBr$_2$(E,F)

3.4 DISCUSSION

The present study incorporated calcium bromide as a potential anti-biofilm compound into BG composition, which for the first time has been explored in tissue engineering applications. Accordingly, the results of this study has supported the hypothesis that BG modified with calcium bromide is able to inhibit different bacteria in multi-species oral biofilm revealed by real time q-PCR analysis. This study demonstrated an appropriate chemical and bimodal size distribution of BG particles and that BG samples embedding 5wt% CaBr$_2$ had an anti-biofilm effect against early, beneficial and pathogen oral biofilm species.

BG embedding 5wt% CaBr$_2$ had a notorious anti-biofilm effect against species such as *S. mitis, S. gordonii, A. viscosus, V. parvula*, and, *P. gingivalis.* Conversely, no biofilm inhibition was distinguished for BG samples embedding 10wt% CaBr$_2$, probably due to the higher roughness values revealed by the discs surfaces corresponding to this

experimental group. A high roughness seemed to affect negatively the anti-biofilm potential. Previous studies have reported that surfaces with higher roughness have more compatibility with biofilm adherence because bacteria is sheltered against shear forces. Additionally, biofilm adhesion area increases with the increment of roughness, which allows biofilm accumulation [39–41]. SEM analysis of biofilm adherence in the disk samples of this study did not show differences between the control and experimental groups; nevertheless, this is a qualitative analysis which only reveals the presence of certain species and is not as precise as q-PCR analysis.

Furthermore, tissue engineering has been challenged to improve BG chemical composition considering biocompatibility and antibacterial effects. In the present study, the crystalline phases analysis revealed the presence of bioactive phases for bone healing such as tetracalcium phosphate and dicalcium silicate [32,34,37]. Regarding BG58S 5wt% $CaBr_2$ processed at 1150 ºC, the XRD spectra (Fig 5) also revealed the presence of phosphorus bromide. Phosphorus tribromide is a compound used in pharmacology as an active compound of anti-inflammatory, analgesic and antipyretic reactions. Also, BG58S $CaBr_2$ 5wt% presented the crystal microstructures typical from calcium phosphates phases, which is an indication of a high bioactivity.

Several previous studies have shown suitable antibacterial properties achieved by bioactive glasses doped with diverse oxides [10-12]. However, possible toxic effects caused by metallic ions and particles embedded into BG are still a controversial concern for clinical applications. Most studies have tested antibacterial properties of modified bioactive glasses against planktonic bacteria solely [7,15,42]. Goh et al. reported that BG samples modified with 5 and 10 mol% cerium oxide demonstrated a significant antibacterial activity against *E. coli*, evaluated by the quantitative viable count method [14]. Additionally, El-Kady et al. established in their study that all BG nanoparticles doped with 1, 3, 5, and 10wt% Ag_2O had antibacterial effect against *S. aureus* and *E. coli* cultures evaluated by the disk diffusion method. That study attributed the high effective antibacterial effect to the presence of silver ions [13]. In contrast, Fooladi et al. stated that silver is not an essential component for inhibiting bacterial growth [24]. That study incorporated MgO into BG nanopowders and its antibacterial effect was assessed against *E. coli*, *P. aureginosa*, and *S. aureus*. The BG nanopowders at a greater concentration than 15.62 mg/mL showed efficient inhibitory effects on the three bacterial strains. As well, selenium nanoparticles have also being added to BG as an

antibacterial agent. Stevanovic et al. showed in their study that BG 45S5 with selenium nanoparticles had a significant antibacterial activity against *S. aureus* and *S. epidermis* cultures, and inhibited *B. subtilis* and *K. pnuemoniae* growth [23]. Fluorine has also being added to BG particles as an antimicrobial agent. Xu et al. showed in their study that BG particles mixed with sodium fluoride (NaF) had a significant *S. mutans* biofilm inhibition effect after 24 hours of exposure. That study tested the anti-biofilm effect against one oral bacteria (monospecie biofilm); nevertheless, currently there are not enough studies testing modified bioactive glass against multi-species oral biofilms. Fluorides are known to inhibit bacterial enzymes like enolase and catalase. Also, compounds with fluorine may disrupt bacterial cell membranes and cytoplasm pH, and interfere glycolysis of cariogenic bacteria [15]. Bromine has many similar characteristics to fluorine although bromine has not being incorporated into BG composition as an antibiofilm agent in previous studies. Considering a lack of findings on the effect of Br based compounds, this study pursued the objective of testing bromide doped BG as a new repairing biomaterial to inhibit multispecies oral biofilm.

The results of the present study are promising since bromide had an anti-biofilm effect against early, beneficial, and pathogen oral species. Nevertheless, future studies evaluating anti-biofilm properties of $CaBr_2$ doped BG samples should take in consideration that samples characteristics, such as surface roughness are of extreme importance regarding biofilm adherence. One limitation of the present study was that samples of the tested groups had different surface roughness values; consequently, biofilm inhibition was evaluated under different circumstances in each study group.

In addition, forthcoming studies should evaluate the biocompatibility and the hydroxyapatite formation capability of innovative bromide doped BG to be tested in future *in vivo* studies. Regarding the mechanism in which bromine acts as anti-biofilm agent, new studies should analyze how bromine ions are able to affect biofilm formation and additionally include clinical strains isolated from patients reporting infection in implanted sites to mimic conditions that are more realistic to clinical complications.

3.5 CONCLUSION

Within the limitations of this study, the main outcomes of this work are drawn as follow:

- The chemical composition of the $CaBr_2$-doped bioactive was monitored and therefore the powder particles showed an angular shape and bimodal size distribution. That plays an important role on the clinical application in bone defects;

- Considering microbiological assessment, bioactive glass doped with 5wt% $CaBr_2$ had a considerable anti-biofilm effect against oral bacteria involved in a multi-species biofilm. Such findings are more representative concerning the aggregation pathways among different species when compared to mono-species methods related in literature. In fact, biomaterials embedding potential antibiofilm compounds must be tested against multi-species biofilms as reported in the present study

- $CaBr_2$-doped bioactive glass can be considered an advantageous anti-biofilm biomaterial for clinical applications and treatment of oral infections at implanted surgical sites. Notwithstanding, other bromide contents and compositions should be assessed by physicochemical and biological tests in further studies to clarify the anti-biofilm behavior of such enhanced bioactive glasses.

3.6 REFERENCES

[1] J.R. Jones, Review of bioactive glass: From Hench to hybrids, Acta Biomaterialia. 9 (2013) 4457–4486. doi:10.1016/j.actbio.2012.08.023.

[2] L.L. Hench, J.R. Jones, Bioactive Glasses: Frontiers and Challenges., Frontiers in Bioengineering and Biotechnology. 3 (2015) 194. doi:10.3389/fbioe.2015.00194.

[3] A. Hoppe, N.S. Güldal, A.R. Boccaccini, A review of the biological response to ionic dissolution products from bioactive glasses and glass-ceramics, Biomaterials. 32 (2011) 2757–2774. doi:10.1016/j.biomaterials.2011.01.004.

[4] P. Sepulveda, J.R. Jones, L.L. Hench, In vitro dissolution of melt-derived 45S5 and sol-gel derived 58S bioactive glasses., Journal of Biomedical Materials Research. 61 (2002) 301–11. doi:10.1002/jbm.10207.

[5] H. Wang, S. Zhao, X. Cui, Y. Pan, W. Huang, S. Ye, S. Luo, M.N. Rahaman, C. Zhang, D. Wang, Evaluation of three-

dimensional silver-doped borate bioactive glass scaffolds for bone repair: Biodegradability, biocompatibility, and antibacterial activity, Journal of Materials Research. 30 (2015) 2722–2735. doi:10.1557/jmr.2015.243.

[6] M.N. Rahaman, B.S. Bal, W. Huang, Review: emerging developments in the use of bioactive glasses for treating infected prosthetic joints., Materials Science & Engineering. C, Materials for Biological Applications. 41 (2014) 224–31. doi:10.1016/j.msec.2014.04.055.

[7] A.M. El-Kady, A.F. Ali, R.A. Rizk, M.M. Ahmed, Synthesis, characterization and microbiological response of silver doped bioactive glass nanoparticles, Ceramics International. 38 (2012) 177–188. doi:10.1016/j.ceramint.2011.05.158.

[8] Z.-P. Xie, C.-Q. Zhang, C.-Q. Yi, J.-J. Qiu, J.-Q. Wang, J. Zhou, In vivo study effect of particulate Bioglass® in the prevention of infection in open fracture fixation, Journal of Biomedical Materials Research - Part B Applied Biomaterials. 90 (2009) 195–201. doi:10.1002/jbm.b.31273.

[9] D. Davies, Understanding biofilm resistance to antibacterial agents., Nature Reviews. Drug Discovery. 2 (2003) 114–22. doi:10.1038/nrd1008.

[10] A. Dongari-Bagtzoglou, Pathogenesis of mucosal biofilm infections: challenges and progress., Expert Review of Anti-Infective Therapy. 6 (2008) 201–8. doi:10.1586/14787210.6.2.201.

[11] M. Gubler, T.J. Brunner, M. Zehnder, T. Waltimo, B. Sener, W.J. Stark, Do bioactive glasses convey a disinfecting mechanism beyond a mere increase in pH?, International Endodontic Journal. 41 (2008) 670–678. doi:10.1111/j.13652591.2008.01413.x.

[12] M.E. Olson, H. Ceri, D.W. Morck, A.G. Buret, R.R. Read, Biofilm bacteria: Formation and comparative susceptibility to antibiotics, Canadian Journal of Veterinary Research. 66 (2002) 86–92.

[13] A.M. El-Kady, A.F. Ali, R.A. Rizk, M.M. Ahmed, Synthesis, characterization and microbiological response of silver doped bioactive glass nanoparticles, Ceramics International. 38 (2012) 177–188. doi:10.1016/j.ceramint.2011.05.158.

[14] Y.F. Goh, A.Z. Alshemary, M. Akram, M.R. Abdul Kadir, R. Hussain, In-vitro characterization of antibacterial bioactive glass containing ceria, Ceramics International. 40 (2014) 729–737. doi:10.1016/j.ceramint.2013.06.062.

[15] Y.-T. Xu, Q. Wu, Y.-M. Chen, R.J. Smales, S.-Y. Shi, M.-T. Wang, Antimicrobial effects of a bioactive glass combined with fluoride or triclosan on Streptococcus mutans biofilm., Archives of Oral Biology. 60 (2015) 1059–1065. doi:10.1016/j.archoralbio.2015.03.007.

[16] M.E. Galarraga-Vinueza, J. Mesquita-Guimarães, R.S. Magini, J.C.M. Souza, M.C. Fredel, A.R. Boccaccini, Anti-biofilm properties of bioactive glasses embedding organic active compounds, Journal of Biomedical Materials Research Part A. (2016) 672–679. doi:10.1002/jbm.a.35934.

[17] J.C.M. Souza, R.R.C. Mota, M.B. Sordi, B. Bernardo, Biofilm Formation on Different Materials Used in Oral Rehabilitation, 27 (2016) 141–147. doi:10.1590/0103-6440201600625.

[18] J.G. Xavier, T.C. Geremias, J.F.D. Montero, B.R. Vahey, C.A.M. Benfatti, J.C.M. Souza, R.S. Magini, A.L. Pimenta, Lactam inhibiting Streptococcus mutans growth on titanium, Materials Science & Engineering C. 68 (2016) 837– 841. doi:10.1016/j.msec.2016.07.013.

[19] S. Clais, G. Boulet, M. Kerstens, T. Horemans, W. Teughels, M. Quirynen, E. Lanckacker, I. De Meester, A.-M. Lambeir, P. Delputte, L. Maes, P. Cos, Importance of biofilm formation and dipeptidyl peptidase IV for the pathogenicity of clinical Porphyromonas gingivalis isolates., Pathogens and Disease. 70 (2014) 408–13. doi:10.1111/2049-632X.12156.

[20] F. Carrouel, S. Viennot, J. Santamaria, P. Veber, D. Bourgeois, Quantitative Molecular Detection of 19 Major Pathogens in the Interdental Biofilm of Periodontally Healthy Young Adults., Frontiers in Microbiology. 7 (2016) 840. doi:10.3389/fmicb.2016.00840.

[21] O. Lysenko, O. Dubok, A. Borysenko, O. Shinkaruk, The biological properties of the silver- and copper-doped ceramic biomaterial, Journal of Nanoparticle Research. 17 (2015). doi:10.1007/s11051-015-2971-z.

[22]   V. Anand, K.J. Singh, K. Kaur, Evaluation of zinc and magnesium doped 45S5 mesoporous bioactive glass system for the growth of hydroxyl apatite layer, Journal of Non-Crystalline Solids. 406 (2014) 88–94. doi:10.1016/j.jnoncrysol.2014.09.050.

[23]   M. Stevanović, N. Filipović, J. Djurdjević, M. Lukić, M. Milenković, A. Boccaccini, 45S5Bioglass®-based scaffolds coated with selenium nanoparticles or with poly(lactide-co-glycolide)/selenium particles: Processing, evaluation and antibacterial activity, Colloids and Surfaces B: Biointerfaces. 132 (2015) 208– 215. doi:10.1016/j.colsurfb.2015.05.024.

[24]   A.A. Imani Fooladi, H.M. Hosseini, F. Hafezi, F. Hosseinnejad, M.R. Nourani, Sol-gel-derived bioactive glass containing SiO2-MgO-CaO-P 2O5 as an antibacterial scaffold, Journal of Biomedical Materials Research - Part A. 101 A (2013) 1582– 1587. doi:10.1002/jbm.a.34464.

[25]   N. Izutani, S. Imazato, K. Nakajo, N. Takahashi, Y. Takahashi, S. Ebisu, R.R.B. Russell, Effects of the antibacterial monomer 12methacryloyloxydodecylpyridinium bromide (MDPB) on bacterial viability and metabolism., European Journal of Oral Sciences. 119 (2011) 175–81. doi:10.1111/j.1600-0722.2011.00817.x.

[26]   J. Mesquita-Guimaraes, M.A. Leite, J.C.M. Souza, B. Henriques, F.S. Silva, D. Hotza, A.R. Boccaccini, M.C. Fredel, Processing and strengthening of 58S bioactive glass-infiltrated titania scaffolds, Journal of Biomedical Materials Research - Part A. (2016) 590–600. doi:10.1002/jbm.a.35937.

[27]   G. Alvarez, M. González, S. Isabal, V. Blanc, R. León, Method to quantify live and dead cells in multi-species oral biofilm by real-time PCR with propidium monoazide., AMB Express. 3 (2013) 1. doi:10.1186/2191-0855-3-1.

[28]   Qiagen, PCR Protocols & Applications - QIAGEN, (n.d.).

[29]   L.R. Rodrigues, M.S. De Laranjeira, M.H. Fernandes, F.J. Monteiro, C.A. De Carvalho Zavaglia, HA/TCP scaffolds obtained by sucrose crystal leaching method: Preliminary in vitro evaluation, Materials Research. 17 (2014) 811–816. doi:10.1590/S1516-14392014005000082.

[30] Z. Sheikh, S. Najeeb, Z. Khurshid, V. Verma, H. Rashid, M. Glogauer, Biodegradable materials for bone repair and tissue engineering applications, Materials. 8 (2015) 5744–5794. doi:10.3390/ma8095273.

[31] S. Joughehdoust, S. Manafi, Synthesis and in vitro investigation of sol-gel derived bioglass-58S nanopowders, Materials Science-Poland. 30 (2012) 45–52. doi:10.2478/s13536-012-0007-2.

[32] M. Taghian Dehaghani, M. Ahmadian, M. Fathi, Synthesis, Characterization, and Bioactivity Evaluation of Amorphous and Crystallized 58S Bioglass Nanopowders, International Journal of Applied Ceramic Technology. 874 (2014) 867–874. doi:10.1111/ijac.12293. This article is protected by copyright. All rights reserved.

[33] M. a. Encinas-romero, S. Aguayo-Salinas, S.J. Castillo, F.F. Castillón-Barraza, V.M. Castaño, Synthesis and characterization of hydroxyapatite-wollastonite composite powders by sol-gel processin, International Journal of Applied Ceramic Technology. 5 (2008) 401–411. doi:10.1111/j.1744-7402.2008.02212.x.

[34] M.A. Encinas-romero, J. Peralta-haley, J.L. Valenzuela-garcía, Synthesis and Structural Characterization of Produced by an Alternative Sol-Gel Route, 2013 (2013) 327–333.

[35] O.M. Goudouri, X. Chatzistavrou, E. Kontonasaki, N. Kantiranis, L. Papadopoulou, K. Chrissafis, K.M. Paraskevopoulos, Study of the Bioactive Behavior of Thermally Treated Modified 58S Bioactive Glass, Key Engineering Materials. 396–398 (2009) 131–134. doi:10.4028/www.scientific.net/KEM.396398.131.

[36] M.M. Obeid, Crystallization of Synthetic Wollastonite Prepared from Local Raw Materials, International Journal of Materials and Chemistry. 4 (2014) 79–87. doi:10.5923/j.ijmc.20140404.01.

[37] W. Lu, W. Duan, Y. Guo, C. Ning, Mechanical properties and in vitro bioactivity of Ca5(PO4)2SiO4 bioceramic., Journal of Biomaterials Applications. 26 (2012) 637–50. doi:10.1177/0885328210383599.

[38] P. Gao, H. Zhang, Y. Liu, B. Fan, X. Li, X. Xiao, P. Lan, M. Li, L. Geng, D. Liu, Y. Yuan, Q. Lian, J. Lu, Z. Guo, Z. Wang, Beta-tricalcium phosphate granules improve osteogenesis in vitro and establish innovative osteo-regenerators for bone tissue

engineering in vivo., Scientific Reports. 6 (2016) 23367. doi:10.1038/srep23367.

[39]   W. Teughels, N. Van Assche, I. Sliepen, M. Quirynen, Effect of material characteristics and/or surface topography on biofilm development., Clinical Oral Implants Research. 17 Suppl 2 (2006) 68–81. doi:10.1111/j.16000501.2006.01353.x.

[40]   M. Quirynen, C.M. Bollen, The influence of surface roughness and surface-free energy on supra- and subgingival plaque formation in man. A review of the literature., Journal of Clinical Periodontology. 22 (1995) 1–14. This article is protected by copyright. All rights reserved. 22

[41]   C.M. Bollen, P. Lambrechts, M. Quirynen, Comparison of surface roughness of oral hard materials to the threshold surface roughness for bacterial plaque retention: a review of the literature., Dental Materials : Official Publication of the Academy of Dental Materials. 13 (1997) 258–69.

[42]   Y.-F. Goh, A.Z. Alshemary, M. Akram, M.R. Abdul Kadir, R. Hussain, Bioactive Glass: An In-Vitro Comparative Study of Doping with Nanoscale Copper and Silver Particles, International Journal of Applied Glass Science. 5 (2014) 255–266. doi:10.1111/ijag.12061. This article is protected by copyright. All rights reserved.

4 ARTIGO 3 EM INGLÊS

O artigo a seguir será submetido na revista científica *Journal of Biomedical materials research: part A*. Fator de impacto: 3.263. Qualis: A1

Mesoporous bioactive glass embedding propolis and cranberry antibiofilm compounds

M.E. Galarraga-Vinueza[1], J. Mesquita-Guimarães[2], R. S. Magini[1], J. C. M. Souza[1,2], M. C. Fredel[2], A. R. Boccaccini[3*]

[1]Center for Education and Research on Dental Implants (CEPID), Post-Graduation Program in Dentistry (PPGO), Department of Dentistry (ODT), Federal University of Santa Catarina(UFSC), Florianopolis/SC, 88040-900, Brazil
[2]Ceramic and Composite Materials Research Group (CERMAT), Federal University of Santa Catarina, Florianopolis 88040-900, Brazil
[3]Institute of Biomaterials, Department of Materials Science and Engineering, University of Erlangen-Nuremberg, 91058 Erlangen, Germany

Corresponding author: A.R. Boccaccini; e-mail: aldo.boccaccini@ww.uni-erlangen.de

Abstract:

Bioactive glasses are attractive materials for bone repairing procedures due to their desirable osteoconductive, angiogenic, osteogenic, and antibacterial properties. In addition, the antibacterial properties of bioactive glass can be enhanced depending on the glass porous structure and chemical composition. The aim of the present study was to evaluate the chemical reactivity of 58S mesoporous bioactive glass free or embedding propolis and cranberry antibiofilm compounds at different concentrations. Mesoporous 58S bioactive glass (MBG) was synthesized by alkali sol-gel method with the addition of the triblock pluronic copolymer P123 as surfactant. Samples were characterized by physco-chemical properties measurement, N_2 adsorption/desorption analysis, and field emission scanning electron microscopy (FESEM) observations. MBG powders were immersed into 5 and 10 μg/ml propolis or cranberry solutions for 24 h. The chemical reactivity of the specimens was evaluated by FESEM, EDX, FTIR and Ca/P analysis after being immersed in simulated body fluid (SBF) solution for 8, 24

and 72 h. MBGs had the expected chemical composition with a particle size distribution ranging from 1.44 up to 955 μm, and a mean particle size of 154 μm. MBG particles exhibited a pore volume of 0.8 cc/g, a pore radius of about 2 nm and a surface area at 350.2 m^2/g, according to BJH and BET analyses. A hydroxyl-carbonate apatite (HCAp) layer was formed on all samples after SBF immersion for 72 h. Pure MBG showed the highest chemical reactivity after 72 h and therefore the resulting apatite layer revealed a Ca/P ratio of 1.8, corresponding to non-stoichiometric biological apatite. MGB embedding propolis and cranberry can be considered for future microbiological analysis since their modified composition did not interfere with the ability of MBG to develop a HCAp layer on its surface, which is an essential property for bone regeneration applications.

Key words: mesoporous bioactive glass, anti-biofilm, sol-gel synthesis, bioactivity, propolis, cranberry PACS, bone healing

4.1 INTRODUCTION

More than 45 years ago, Hench et al. developed the first bioactive glass (BG) of composition: (46.1 mol.% SiO_2, 24.4 mol.% Na_2O, 26.9 mol.% CaO and 2.6 mol.% P_2O_5); with the purpose of generating a biomaterial that could bond to bone fulfilling the requirements of orthopedic surgeries of the time[1]. After many years of bioactive glass intensive research, BGs have been demonstrated to be outstanding materials due to their desirable characteristics such as high bioactivity, osteogenic stimulation, angiogenic effect, ability to bond to soft tissues, high biocompatibility and antibacterial activity induced by its ion release capability [2–10]. It is well established that highly bioactive synthetic glasses bond to bone through the formation of a hydroxyl-carbonate apatite (HCAp) layer which mimics the mineral phase of bone; thus, resulting in a biological match between BGs and bone tissues [3,10]. Certainly, bioactivity accomplished through a high chemical reactivity in contact with human tissues is the most acclaimed property of bioactive glasses; nevertheless, new tissue engineering requirements have emerged besides this property to fulfill the necessities of surgical and regenerative procedures which include also applications in soft tissue repair [6,7,9].

Several new BG compositions have been developed over the years to improve bioactivity and mechanical properties[6,10]. Recent advances have considered BG structures characterized by nano-porous organized arrangements, known as mesoporous bioactive glass (MBG),

which are developed by the sol-gel method [11–14]. MBGs exhibit large surface area with organized nano-porous channels which can induce a higher HCAp formation and allow the incorporation of bioactive molecules such as bone morphogenetic proteins (BMP) and vascular endothelial growth factor (VEGF) to induce osteogenesis and angiogenesis [12,14]. Furthermore, MBGs can act as drug delivery systems by the incorporation and release of antibiotics, antibacterial and antibiofilm compounds in their nano porous structure [11,12,14,15].

Studies have reported that orthopedic and craniofacial surgeries have a considerable risk of postoperative bone infection and that bone implant associated infections are major complications of bone repairing procedures [4,5,16–18]. Systemic antibiotic therapy is the most common treatment of bone-associated infections. However, such therapy can cause a bacterial resistance of pathogenic species considering the formation of biofilms [14]. It should be highlighted that biofilms consist of a well-organized microbial community embedded in an extracellular polymeric matrix composed of polysaccharides, nucleic acids, proteins and water being the main cause of implanted bone infections [17,19,20]. Bacteria organized in a multispecies biofilm is 1000 times more resistant to antibiotics when compared to planktonic bacteria [19]. Thus, BGs have been considered as favorable biomaterials to locally counteract grafted or implanted site infections due to their antibacterial effect accomplished by raising the pH of the medium, which affects planktonic bacterial growth [8]. Only few studies have reported the effect of BG on multispecies biofilm as found in the oral cavity [4,21]. Several antibiotics such as gentamicin, teicoplanin, tetracycline, vancomycin, and cefuroxime axetil [22–26] have being loaded into MBGs leading to favorable antibacterial effects. However, the antibiofilm effect of MBG loaded with antibiotics has not been completely validated in these studies. Hence, it is of clinical relevance to incorporate antibiofilm rather than antibacterial compounds into MBG for an effective infection treatment [27].

Previous studies have reported the incorporation of natural derived antibiofilm compounds into BG and MBG [28–30]. Surface functionalization of BGs has been explored for the incorporation of natural biomolecules such as polyphenols, which have potential antibacterial benefits[30]. Additionally, a herbal derived substance called propolis, which is a resinous natural substance collected by bees, has being described to have several health promoting properties like fibroblast stimulation, antioxidant activity, antifungal and antiviral activity, antibiofilm inhibition and counteraction of bacteria virulent

factors [29,31]. Propolis has shown non-cytotoxic effects, but it has not been deeply explored in tissue engineering applications [32,33]. Only one study [29] has incorporated red and green propolis collected from different regions into BG, showing a satisfactory growth inhibition of *S. aureus, E. faecalis, S. mutans, P. intermedia, F. nucleatum, P. gingivalis,* and, *A. actinomycetemcomitans.* Moreover, other natural compounds, such as A-type proanthocyanidins (PACS) derived from the cranberry fruit (*Vaccinium macrocarpon*) have also demonstrated a potential antibiofilm effect[34]. Initially, cranberry PACS were widely studied to prevent and treat urinary tract infections since they prevent bacterial adhesion to uroepithelial cells [34,35]. Additionally, Kim et al. reported that PACS are capable of inhibiting bacterial adhesion on the exopolysaccharide (EPS) matrix which provides biofilm mechanical stability for microbial proliferation [36]. Other studies have also shown that cranberry PACS neutralize *S. mutans* virulence factors and increase the medium pH leading to changes of biochemical and ecological factors for cariogenic biofilm development [37,38]. On the other hand, even though several studies have reported the antibiofilm potential of cranberry PACS[34–38], that compound has not been incorporated into biomaterials to treat bone-derived infections and for bone regeneration.

Accordingly, this study pursuits to integrate natural derived antibiofilm substances in bioactive glasses. In particular, a novel mesoporous bioactive glass incorporating propolis and cranberry antibiofilm compounds was developed. The hypothesis behind this work is that the incorporation of propolis and cranberry compounds will not affect the inherent bioactivity of 58S mesoporous bioactive glass, developing thus a material , which is both effective against biofilm formation and suitable to bond to bone without addition of antibiotic drugs.

4.2 MATERIALS AND METHODS

4.2.1 MBG sol-gel synthesis

MBG (58 wt% SiO_2, 33 wt% CaO, 9 wt% P_2O_5) (58S composition) powder was processed via a sol-gel technique. First, 4 g of pluronic triblock copolymer P123 (EO20PO70EO20, 5800, Sigma Aldrich, USA) surfactant was dissolved in 50 mL ethanol by using a stirring bar at 40 °C for 1 h. Afterwards, tetraethyl orthosilicate (TEOS) (98%, Sigma Aldrich, USA), triethyl phosphate (TEP) (99.8%, Sigma Aldrich, USA) and calcium nitrate tetrahydrate ($Ca(NO_3)_2 \cdot 4H_2O$)

(Vetec, Brazil) were added to the solution as precursors of silicon, phosphorous and calcium oxide. The solution was stirred at $40°C$ for 12 h. Nitric acid (HNO_3, 68%, Vetec, Brazil) was used to dissolve $Ca(NO_3)_2 \cdot 4H_2O$ and to adjust the pH of the solution while ethyl alcohol (EtOH, P.A., Synth, Brazil) was used to dissolve P123, TEOS and TEP. The molar ratios of SiO_2, P_2O_5 and CaO were calculated, concerning the 58S MBG proportion. TEOS and TEP were placed in a glass recipient containing EtOH under magnetic stirring at 25 $°C$ for 10 min. $Ca(NO_3)_2 \cdot 4H_2O$ was dissolved in 2 M HNO_3 and then added to water at a molar ratio TEOS:H_2O of 1:4. Then, the solution was placed for drying in a chamber at 70 °C over a period of 24 h. Subsequently, the dried gel was thermally treated at 600 °C for 6 h at a heating rate of 1°C/min to remove the organic agents and the surfactant template. The methodology used in this study is schematically shown in Figure 1.
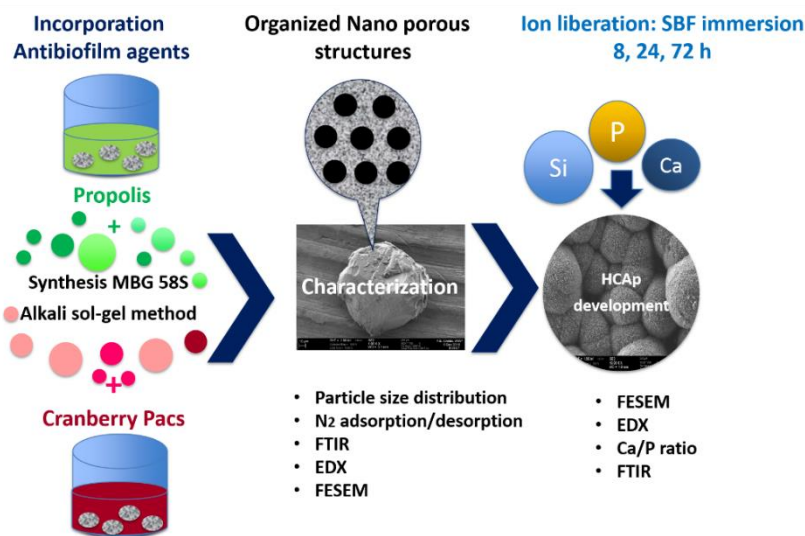
Figure 1. Schematic diagram showing the methodology applied in this study to prepare MBG incorporating propolis and cranberry PACS.

4.2.2 Physicochemical characterization

The particle size distribution was measured in a laser diffraction equipment (Mastersizer 2000, Malvern, UK). The powder was introduced in a wet dispersion unit with low water rotation (~1200 rpm) to avoid significant agglomeration of the particles.

Chemical analysis of the samples was performed using energy dispersive X-ray spectroscopy (EDX, Swift 2000, Hitachi, Japan). The compound composition was obtained by rearranging the quantity of oxygen to calculate the weight percentage of oxides using the most stable stoichiometric arrangement, resulting in a reliable tool to semi-quantify the respective oxides. The functional groups of the powder samples were identified by Fourier transform infrared spectroscopy (FTIR, Cary 600 Series, Agilent technologies, USA), performed by KBr pellet technique. Pellets were prepared by mixing 1 mg of each sample powder and 300 mg KBr at infrared grade under vacuum. The infrared spectra were recorded in a wavenumber of 400-4000 cm^{-1} in transmission mode with 32 scans and resolution of 4 cm^{-1}.

MBG textural analysis was performed by N_2 adsorption and desorption isotherms measured by a porosity analyzer (AUTOSORB-1-1 C, Quantochrome) at -203.85°C. Pore size distribution and volume were determined from the isotherm adsorption branch applying the Barrett-Joyner-Halenda (BJH) method while the surface area was established by the Brunauer-Emmett-Teller (BET) method. The morphologic aspects of the MBG particles were analyzed by field emission gun scanning electron microscopy (FESEM) (Zeiss Leica, Germany) at an acceleration potential of 5 kV.

4.2.2 *In vitro* loading of propolis and cranberry compounds

Green propolis dry extracts from *Baccharis dracunculifolia* sp. (Natucentro®, Minas Gerais, Brazil) and Cranberry PAC dry extracts from *Vaccinium macrapon* sp. (Naturex-DBS® , Massachusetts, USA) were diluted in a 50% (v/v) hydro-alcoholic solution (EtOH, P.A., Synth, Brazil) under magnetic stirring at room temperature for 5 h to prepare solutions of 5 and 10 μg/mL as described in a previous study [31]. Then, 0.5 g of MBG powders were immersed into 50 mL of the corresponding solutions with different concentrations and stirred at 37°C for 24 h. MBG powders were also added into a hydro-alcoholic solution free of natural derived compounds to prepare the control group. After immersion, the solutions containing MBG powders were centrifuged and dried in a vacuum oven at 40 °C for 3 h.

4.2.3 *In vitro* apatite-forming assays

Simulated body fluid (SBF) solution was prepared following Kokubo´s method [39]. The chemical composition of the SBF solution is shown in Table 1. MBG powders (75 mg) were immersed into 50 mL

of SBF solution in sterilized PS flasks. The flasks were placed in an incubator (IKA, Germany) at 37°C and stirred at 90 rpm for 8, 24 or 72 h. At the end of each period, the samples were centrifuged, removed by filtration, washed with deionized water and dried in a vacuum oven at 37°C for 24 h [40]. Each sample was run in triplicate. Afterwards, the HCAp-forming ability of all samples was evaluated by SEM, EDX, and FTIR analysis.

Table 1. Chemical composition of the SBF stock solution [40]

ORDER	REAGENT	AMOUNT (g/l)
1	NaCl	8.035
2	NaHCO	0.355
3	KCl	0.225
4	K_2HPO_4 $3H_2O$	0.231
5	$MgCl_2$ $6H_2O$	0.311
6	HCl 1M	38 mL
7	$CaCl_2$ $2H_2O$	0.386
8	Na_2SO_4	0.072
9	Tris	6.118

4.3 RESULTS

4.3.1 Characterization of MBG particles

MBG particle size ranged from 1.44 up to 955 μm, revealing a Gaussian-like distribution, as seen in Figure 2A. The mean particle size was around 154 μm. The actual chemical composition of 58S MBG particles was close to the expected composition (58.22 ± 2 wt% SiO_2, 33.091 ± 3 wt% CaO, 8.6 ± 1 wt% P_2O_5) as shown in Figure 2B. EDX spectra showed the highest intensity peak for the Si element, followed by Ca element and P element (Figure 2B).

The FTIR analysis showed BG characteristic peaks of Si-O-Si where the main absorption bands were at 1080, 810 cm^{-1}, attributed to the Si-O-Si asymmetric stretching, and at 460 cm^{-1} attributed to Si-O-Si bending, as demonstrated in Figure 3.
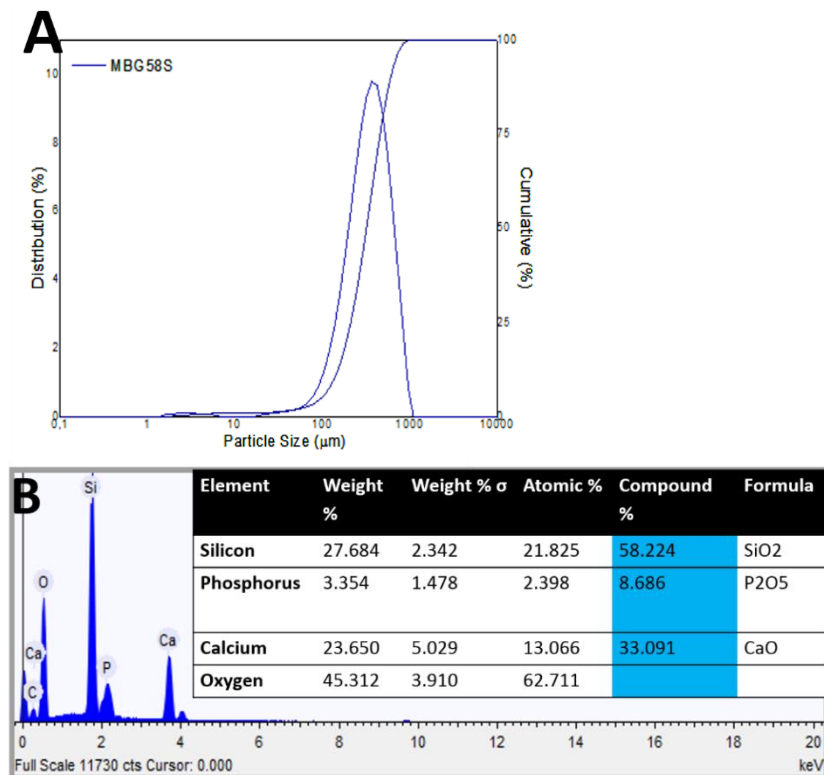
Figure 2. (A) MBG 58S particle size distribution and (B) EDX results for 58S MBG.

The textural analysis regarding N_2 adsorption-desorption isotherms, BJH pore size distribution and volume are shown in Figure 4. 58S MBG N_2 adsorption-desorption isotherms (Figure 4A) corresponded to a type IV curve of the International Union of Pure and Applied Chemistry (IUPAC) classification which is typical of mesoporous materials showing a H1 type hysteresis loop [41]. The initial part of this curve can be associated to monolayer-multilayer adsorption. Also, a limiting uptake in a range of high P/Po was noted[42]. In addition, the sharp steps in adsorption and desorption branches at 0.7-0.8 and 0.6-0.7 P/Po regions respectively, are associated to capillary condensation at mesopores. The BHJ method revealed that MBG particles had a mean narrow pore radius at 2 nm, as shown in Figure 4B, and a porosity volume of about 0.83 cc/g. The MBG specific surface area was 350.2 m^2/g according to BET analysis.
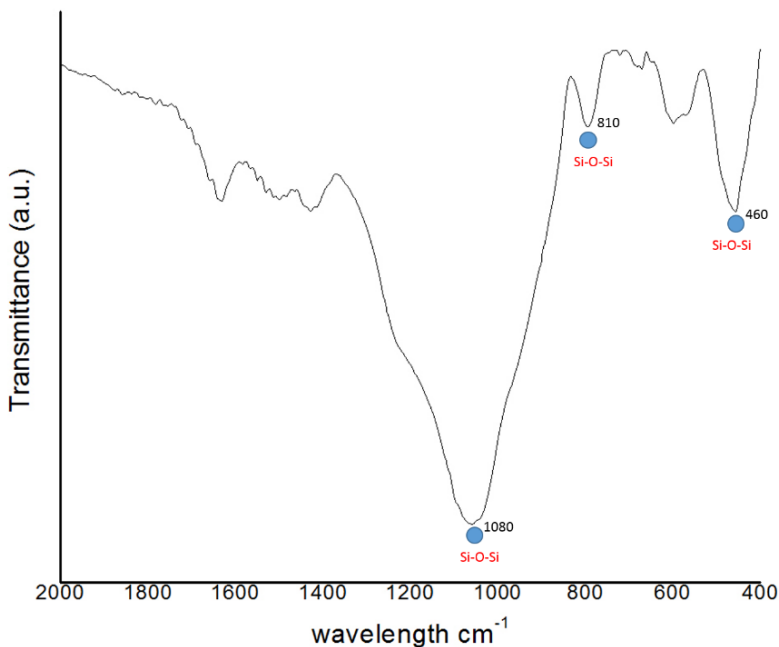
Figure 3. FTIR spectrum obtained for 58S mesoporous bioactive glasses (relevant peaks are indicated).
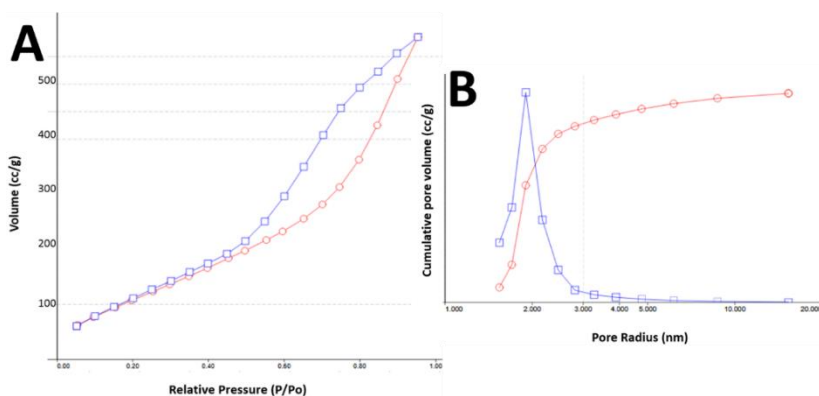
Figure 4. (A) N_2 adsorption (red)-desorption (blue) isotherms and (B) BJH pore radius distribution curves for 58S mesoporous bioactive glass particles.

FESEM micrographs revealed a fairly regular and uniform appearance of MBG particles, as seen in Figure 5A. At higher

magnifications, MBG particles showed an angular shape and non-smooth porous structure, having pores below 10 nm in diameter, as observed in Figure 5B and 5C. Also, sphere-like structures below 100 nm are noticed in Figure 5C, probably indicating crystallized β-Tricalcium phosphate which may have formed after thermal treatment of the samples as described elsewhere [4].

Figure 5. (A-C) FESEM images of 58S MBG 58S particles at different magnifications. In (C) nano-pores (white squares) are revealed at 80,000X magnification.
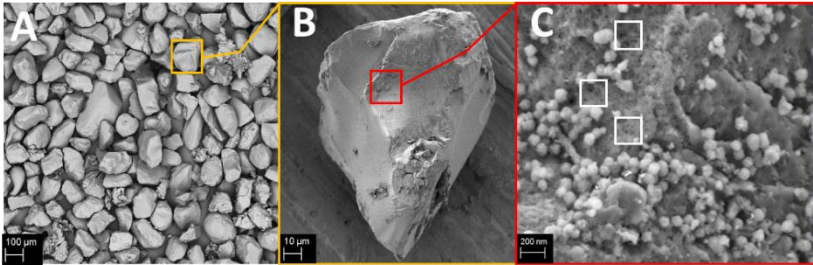
4.3.2 *In vitro* apatite-forming assays

FESEM images revealed that the surface of all samples was relatively smooth and did not exhibit any HCAp formation after immersion in SBF for 8 h (Fig. 6). After 24 h, all MBG samples changed their surface morphology having a more granular-like appeareance. For 72 h of immersion, all samples showed spherical-like structures which indicates the formation of apatite crystals. The control 58S MBG particles showed an apatite layer formed over their surface upon 24 h of immersion in SBF, as seen in Figure 6A whereas almost all MBG particles were covered with an HCAp layer. MBG particle surfaces were covered with a thick HCAp layer revealing spherical, needle, polygonal, and cauliflower-shaped crystals.

In the case of MBG particles embedding 5 µg/ml cranberry PACS, an increase of roughness seemed to take place after 24 h immersion in SBF. Also, the surface was covered with sphere-shaped apatite crystals after 72 h of immersion in SBF, as seen at higher magnification (Figure 6B, white squares). In the case of MBG embedding 10 µg/ml cranberry PACs, the sample surface was still smooth after 24h of immersion when compared to the control group. Only some round plain structures could be detected on MBG embedding 10 µg/ml cranberry (Figure 6C). On FESEM micrographs, MBG

particles embedding 10 µg/ml cranberry showed the lowest HCAp formation after 24 h among all samples. After 72 h of immersion, the surface of MBG embedding 10 µg/ml cranberry was not smooth anymore due to the presence of numerous small rounded apatite structures (Fig. 6C).

MBG particles embedding both propolis concentrations are shown in Figures 6D and 6E. Both samples showed the development of an HCAp layer after 24 h of immersion in SBF that was more noticeable when compared to the other experimental group samples. After 72 h, a cauliflower shaped apatite layer could be clearly detected for both MBG/propolis containing samples, as seen in Figure 6D and 6E at the highest magnification micrographs (white squares).

EDS analyses were performed in triplicate for all samples to determine the Ca/P atomic ratio, as shown in Table 2. The EDS spectra analysis showed non-significant changes in MBG composition for all samples after immersion in SBF for 8 h (Fig. 7). After 24 h, EDS showed an increase in Ca and P wt% while Si wt% decreased in all samples. Generally, MBG samples showed a notorious Si wt% loss and a higher wt% P after immersion in SBF for 72 h. EDS analysis on MBG embedding 5µg/ml propolis revealed Si as the main element followed by Ca and P after immersion in SBF for 8 h (Fig. 7A). However, a decrease in Si content and increase in P and Ca concentrations are noticed after 24 immersion in SBF (Fig. 7B). This result can be linked to the presence of a thick HCAp layer as shown in the SEM micrograph. Finally, after 72h, figure 7C shows an EDS spectrum exhibiting a lower Si wt% and higher P wt% corresponding to the formation of HCAp, which is expected after immersion in SBF for 72 h (Fig. 7C), as seen by SEM micrographs. The Ca/P ratios shown in Table 2 indicate that the unloaded MBG sample reached a Ca/P ratio of 1.8 after immersion in SBF for 72h, which is in accordance to non-stoichiometric HCAp ratio [43]. The samples embedding propolis in both concentrations revealed Ca/P ratios close to the HCAp reference value after 72 h of immersion in SBF. MBG sample embedding 5 µg/ml of cranberry PACs showed a ratio of 2.03 although MBG embedding the higher cranberry PACs concentration had a Ca/P ratio of 2.85.
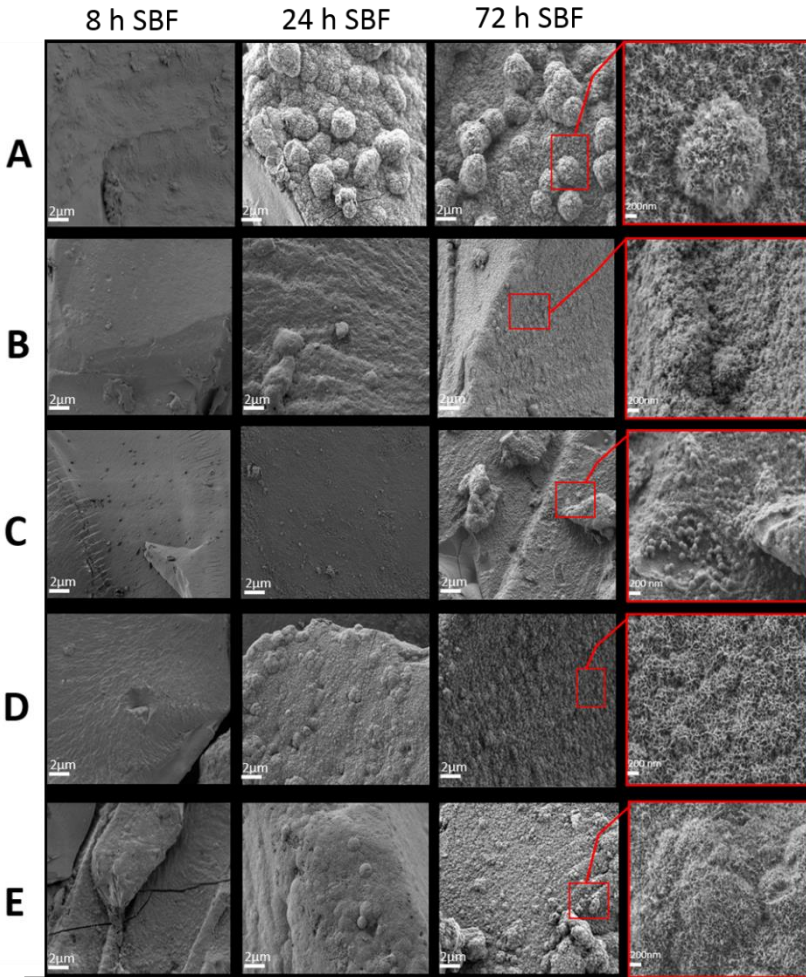
Figure 6.FESEM micrographs at 10,000X recorded on 58S MBG particles after immersion in SBF for 8, 24 and 72 h. MBG (A) Pure and containing (B) 5 µg/ml cranberry PACS, (C) 10 µg/ml cranberry PACs, (D) 5µg/ml propolis and (E) 10 µg/ml propolis. Red squares exhibit corresponding micrographs at 50,000X.
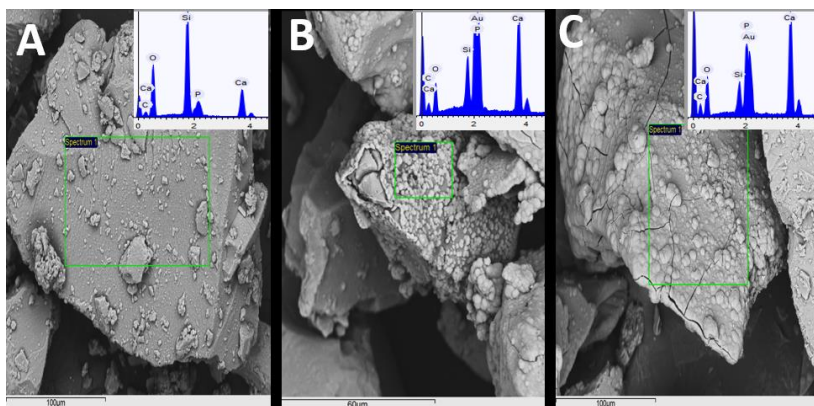
Figure 7. SEM images (1,000X) and EDX analysis recorded on MBG containing 5 µg/ml propolis particles immersed in SBF solution for (A) 8 h, (B) 24 h and (C) 72 h.

Table 2. Ca/P elemental concentration ratio of samples before and after SBF immersion for 0, 8, 24 and 72 h

Time SBF (h)	MBG 58s	MBG/prop 5 µg/ml	MBG/prop 10 µg/ml	MBG/PACS 5 µg/ml	MBG/PACS 10 µg/ml
0	7.16 ± 1	6.67 ± 1	6.56 ± 1,5	8.1 ± 1	7.03 ± 1
8	4.89 ± 2	5.7 ± 2	6.02 ± 1	7.3 ± 1,5	7.01 ± 2.5
24	2.01 ± 1	4.08 ± 1.5	5.08 ± 1	6.04 ± 1	6.07 ± 1.5
72	1.81±1.5	1.9 ± 1.6	2.01 ± 1.5	2.03 ± 2	2.85 ± 1

The samples of the present study after 8 and 24 hours of SBF immersion did not show significant compositional changes in the FTIR spectra. The FTIR spectra of MBG with 5 or 10 µg/ml of propolis and cranberry PACS were similar after 72h of immersion. Figure 8 exhibits the spectra for MBG incorporating 5 µg/ml for both compounds. The FTIR spectra of all samples presented the characteristic peaks attributed to HCAp layer formation as a doublet at around ~600 cm^{-1} corresponding to the bending mode of crystalline phosphate P-O and P-O stretching mode at ~1050 cm^{-1}, where the resonance was more intense especially for the spectrum of pure MBG. On the other hand the spectrum of MBG before SBF immersion indicates the absence of the mentioned double peak. Additionally, resonances attributed to the phosphate group were present in the spectra of pure MBG, MBG/cranberry PACS and MBG/propolis. A narrowing band at around 820 cm^{-1} corresponds to the bending mode of C-O and at around 1400cm^{-1} a

peak corresponding to the C-O stretching mode can also be observed in the pure MBG spectrum. In addition, at ~1680 cm^{-1} the resonance corresponding to C-O in CO_3^{2-} can also be observed indicating the formation of a carbonated HAp due the presence of CO_2 in SBF.
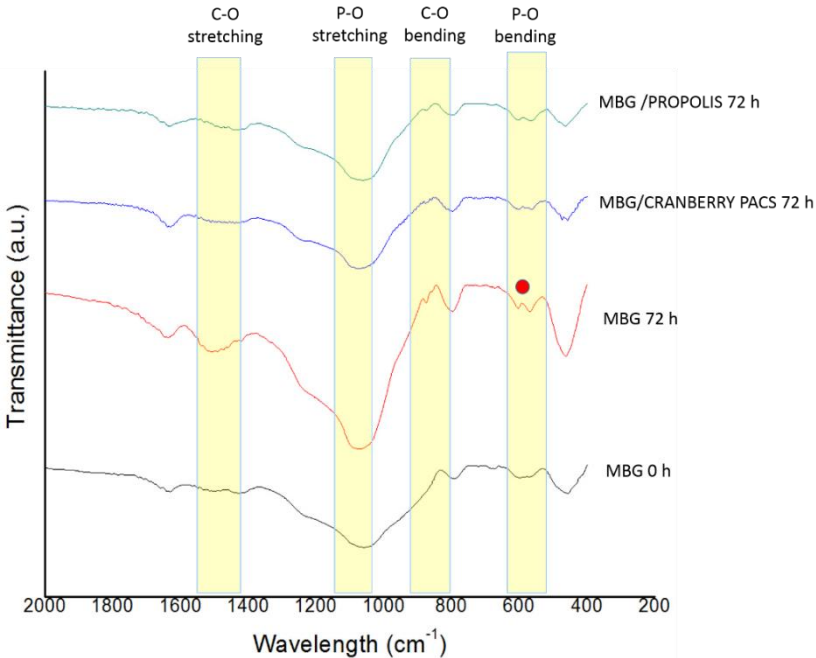
Figure 8. FTIR spectra obtained for 58S mesoporous bioactive glass samples (free MBG, MBG-5 µg/ml propolis and MBG-5 µg/ml cranberry PACS) before and after 72 h of SBF immersion. (Red circle identifies the double peak characteristic of HCAp formation)

4.4 DISCUSSION

The present work synthesized mesoporous bioactive glass incorporating propolis and cranberry compounds in order to enhance the bioactive properties and anti-biofilm potential of MBG for bone healing and infection treatment procedures. The results of the present study supported the hypothesis that natural derived compounds incorporated into MBG did not interfere with the inherent bioactivity of this biomaterial. This study demonstrated an appropriate physical, chemical, and particle size distribution of MBG samples. Moreover, the addition of the surfactant P123 to the sol gel synthesis did not change the

characteristic chemical composition of 58S BG, as confirmed by EDX and FTIR analysis.

Furthermore, the textural analysis showed that the synthesized MBG particles had a meso-porous structure of pore size of 4nm, with a high volume and specific surface area making it capable to incorporate in its structure therapeutic agents as a drug delivery system. The mesoporous structure of the synthesized MBG could be determined by its IV N_2 adsorption and desorption isotherm curve with a H1-type hysteresis loop at high relative pressure according to the IUPAC classification [11,42]. The present study is supported by previous investigations showing the same type of hysteresis loop in the N_2 isotherms for mesoporous materials [12,14,44,45], however in this study the organization and arrangement of the meso-pores were not confirmed (e.g. by TEM). In addition, previous studies developing MBGs have shown higher surface area, pore volume, and pore diameter that should enhance the MBG capability to incorporate therapeutic agents in their nano-structure and favor a higher HCAp formation to bond with bone receptor tissues [46]. A high surface area increases the amount of Si-O bonds to interact with loaded therapeutic agent molecules and a high pore diameter and volume enables a larger space for drug load and sustained delivery. Furthermore, diverse biomolecules such as BMPs and VEGF can covalently bond to MBG surfaces to stimulate specific target cells for osteogenesis and angiogenesis [46,47]. Even though the present study showed appropriate meso-pore characteristics, other structure directing agents could be applied such as F127, F108, P85, CTAB, and P123+CTAB, reported in other studies [12,48], to increase the surface area and volume of MBG improving in this way the mentioned therapeutic, bioactive and osteogenic characteristics [14].

The simulated body fluid test is widely accepted to evaluate the bioactivity of a material in terms of its ability since it mimics the process in which a biomaterial is able to bond to bone tissues through the formation of a bone like apatite layer [39,40]. As follows, the mechanism of MBG apatite formation involves a series of steps. First, an exchange between calcium and hydrogen ions occurs. Consequently, silanol forms over the surface of the biomaterial and polymerizes producing an amorphous silica gel. Afterwards, calcium and phosphate ions migrate to the newly formed silica gel and start forming an HCAp layer, which finally crystallizes forming needle and cauliflower-shaped structures which promote the attachment of bone cells [49]. In this study, MBG free or incorporating propolis and cranberry compounds did not exhibit apatite formation after 8 h in SBF solution; however, all the

samples were able to induce a significant HCAp layer after 72 h in SBF. Additionally, pure MBG samples revealed through chemical and microscopic analysis the greatest HCAp formation after 24 and 72 h, where their surface was completely covered by needle like and cauliflower-shaped crystals typical of the process of HCAp crystallization [43,50,51]. Nevertheless, MBGs immersed in propolis and cranberry solutions were also able to develop an HCAp layer after 72 h. Only the highest concentration of cranberry PACS solution seemed to interfere with the HCAp forming capability of MBG particles. The highest concentration (10 µg/ml) of cranberry PACS negatively affected the bioactivity of the samples which can be observed in FESEM micrographs and Ca/P values comparable to 1.8 which corresponds to non-stoichiometric hydroxyapatite [43]. Furthermore, pure MBG, 5-10 µg/ml propolis and 5µg/ml cranberry MBGs had a Ca/P value close to 1.8 demonstrating the presence of HCAp. In addition, EDX analysis exhibited after 24 and 72 h a notorious increase of calcium and phosphate wt% in all samples indicating the formation of a calcium phosphate layer over MBG particles by the reaction of Ca^{2+} and PO_4^{3-} ions from SBF solution. These results are relevant for the intended applications in bone regeneration, since released Ca, Si and P ions from MBG particles can improve cell proliferation through HCAp layer formation, as reported in previous studies [49,52]. Finally, FTIR analysis did not show any significant change in the chemical composition of the samples after 8 h of SBF immersion. MBG incorporating propolis and cranberry compounds at both concentrations exhibited similar FTIR spectra after 72 h in SBF. As shown in figure 8, FTIR spectra for all samples after 72 h showed characteristic peaks attributed to HCAp layer formation as other studies report [53,54]. Resonance bands attributed to P-O and C-O were observed in all samples especially in pure MBG particles. This chemical analysis supports FESEM observations, which indicated that samples were able to develop an HCAp layer after 72 h of SBF immersion. This observation has clinical relevance since this HCAp layer on MBG surface layers facilitates bone contact few days after the surgical procedure.

BGs have been modified over the years with the incorporation of diverse antibacterial and antibiofilm agents to counteract bone infection. Various studies have reported the incorporation of metal oxides, antibiotics and other organic agents into bioactive glasses[11–16]; however, there is no consensus until present days of which antibiofilm agent is the most effective for bone infection treatment [8,41,55–57].

Indeed, the BG S53P4 is being successfully commercialized to counteract osteomyelitis conditions [58–60]. Taking in consideration that some metal ions have toxic effects in the human body [61], the present study investigated for the first time embedding in MBG two natural derived antibiofilm components consumed by humans which have no toxic effects [33,35]. Propolis and cranberry antibiofilm compounds have complex and rich phytochemical compositions of diverse elements such as flavonoids, steroids, amino acids, phenolic and aromatic compounds, which vary in composition and quantity depending on their growing conditions [62,63]. For this reason, the present study used propolis and cranberry compounds that already had chromatographic analysis and were previously standardized for commercial distribution. A difficulty of this study was to develop a protocol to incorporate propolis and cranberry compounds into bioactive glass mesoporous structures since there are no previous related studies that have followed an established and replicable methodology. Consequently, this study followed standard methods to develop an "accurate" procedure to embed propolis and cranberry compounds into MBG through the immersion technique. In addition, the main objective of the present study was to evaluate the bioactivity of the modified MBGs since this is an essential and desired characteristic of this biomaterial. Further studies are required to understand the mechanisms in which these natural agents bond to MBG surfaces, how its delivery takes place and if their antibiofilm potential is effective to treat bone infections. Certainly, nature´s incomparable properties via antibiofilm compounds can be explored in novel biomaterial combinations, in this case with MBG, to develop a superior biomaterial system able to accomplish tissue-engineering goals with simultaneous anti-infection outcome.

4.5 CONCLUSION

The main conclusions of this study and perspectives for further reserach are the following:

- MBG (58S) exhibited favorable physical properties, especially their mesoporous structure, that can act as a drug delivery system targeting specific areas where therapeutic agents are required, representing an alternative to systemic antibiotic therapy.

- All samples were able to induce an HCAp layer formation on MBG particles after 72 h of SBF immersion, which is important for clinical applications since such HCAp layer on MBG enables bone contact only few days after the grafting procedure.

- The incorporation of propolis and cranberry PACS compounds reported as antibiofilm agents did not inhibit the HCAp formation ability of MBG, thus imparting their antibiofilm properties for bone repair and infection treatment.

- Further studies are needed to assess the effects provided by the antibiofilm agent confined and delivered through MBG nano-pores and to develop release triggers such as pH, temperature, and light, which could make the delivery system more effective and sustained.

Acknowledgements

4.6 REFERENCES

[1]   L.L. Hench, R.J. Splinter, W.C. Allen, T.K. Greenlee, Bonding mechanisms at the interface of ceramic prosthetic materials, J. Biomed. Mater. Res. 5 (1971) 117–141. doi:10.1002/jbm.820050611.

[2]   A. Hoppe, N.S. Güldal, A.R. Boccaccini, A review of the biological response to ionic dissolution products from bioactive glasses and glass-ceramics, Biomaterials. 32 (2011) 2757–2774. doi:10.1016/j.biomaterials.2011.01.004.

[3]   L.L. Hench, Opening paper 2015- Some comments on Bioglass: Four Eras of Discovery and Development, Biomed. Glas. 1 (2015) 1–11. doi:10.1515/bglass-2015-0001.

[4]   M.E. Galarraga-Vinueza, B. Passoni, C.A.M. Benfatti, J. Mesquita-Guimarães, B. Henriques, R.S. Magini, et al., Inhibition of multi-species oral biofilm by bromide doped bioactive glass, J. Biomed. Mater. Res. Part A. (2017). doi:10.1002/jbm.a.36056.

[5]   L. Drago, E. De Vecchi, M. Bortolin, M. Toscano, R. Mattina,
        C.L. Romanò, Antimicrobial activity and resistance selection of
        different bioglass S53P4 formulations against multidrug resistant
        strains, 10 (2015) 1293–1299.

[6]   M.N. Rahaman, D.E. Day, B. Sonny Bal, Q. Fu, S.B. Jung, L.F.
        Bonewald, et al., Bioactive glass in tissue engineering, Acta
        Biomater. 7 (2011) 2355–2373. doi:10.1016/j.actbio.2011.03.016.

[7]   A.A. Gorustovich, J.A. Roether, A.R. Boccaccini, Effect of
        bioactive glasses on angiogenesis: a review of in vitro and in vivo
        evidences., Tissue Eng. Part B. Rev. 16 (2010) 199–207.
        doi:10.1089/ten.TEB.2009.0416.

[8]   M.E. Galarraga-Vinueza, J. Mesquita-Guimarães, R.S. Magini,
        J.C.M. Souza, M.C. Fredel, A.R. Boccaccini, Anti-biofilm
        properties of bioactive glasses embedding organic active
        compounds, J. Biomed. Mater. Res. Part A. 105 (2017) 672–679.
        doi:10.1002/jbm.a.35934.

[9]   V. Miguez-Pacheco, L.L. Hench, A.R. Boccaccini, Bioactive
        glasses beyond bone and teeth: Emerging applications in contact
        with soft tissues, Acta Biomater. 13 (2015) 1–15.
        doi:10.1016/j.actbio.2014.11.004.

[10]   J.R. Jones, Review of bioactive glass: from Hench to hybrids.,
        Acta Biomater. 9 (2013) 4457–86.
        doi:10.1016/j.actbio.2012.08.023.

[11]   Y. Li, Y.Z. Liu, T. Long, X. Bin Yu, T.T. Tang, K.R. Dai, et al.,
        Mesoporous bioactive glass as a drug delivery system:
        Fabrication, bactericidal properties and biocompatibility, J.
        Mater. Sci. Mater. Med. 24 (2013) 1951–1961.
        doi:10.1007/s10856-013-4960-z.

[12]   C. Wu, J. Chang, Mesoporous bioactive glasses: structure
        characteristics, drug/growth factor delivery and bone regeneration
        application, Interface Focus. 2 (2012) 292–306.
        doi:10.1098/rsfs.2011.0121.

[13]   M. Vallet-Regí, E. Ruiz-Hernández, Bioceramics: From Bone
        Regeneration to Cancer Nanomedicine, Adv. Mater. 23 (2011)
        5177–5218. doi:10.1002/adma.201101586.

[14]   C. Wu, J. Chang, Multifunctional mesoporous bioactive glasses

for effective delivery of therapeutic ions and drug/growth factors., J. Control. Release. 193 (2014) 282–295. doi:10.1016/j.jconrel.2014.04.026.

[15] J. Hum, A.R. Boccaccini, Bioactive glasses as carriers for bioactive molecules and therapeutic drugs: a review., J. Mater. Sci. Mater. Med. 23 (2012) 2317–33. doi:10.1007/s10856-012-4580-z.

[16] V. Mourino, A.R. Boccaccini, Bone tissue engineering therapeutics: controlled drug delivery in three-dimensional scaffolds, J. R. Soc. Interface. 7 (2010) 209–227. doi:10.1098/rsif.2009.0379.

[17] J. Geurts, J.J. Chris Arts, G.H.I.M. Walenkamp, Bone graft substitutes in active or suspected infection. Contra-indicated or not?, Injury. 42 Suppl 2 (2011) S82-6. doi:10.1016/j.injury.2011.06.189.

[18] W. Teughels, N. Van Assche, I. Sliepen, M. Quirynen, Effect of material characteristics and/or surface topography on biofilm development., Clin. Oral Implants Res. 17 Suppl 2 (2006) 68–81. doi:10.1111/j.1600-0501.2006.01353.x.

[19] D. Davies, Understanding biofilm resistance to antibacterial agents., Nat. Rev. Drug Discov. 2 (2003) 114–22. doi:10.1038/nrd1008.

[20] A. Mombelli, N. Müller, N. Cionca, The epidemiology of peri-implantitis, Clin. Oral Implants Res. 23 (2012) 67–76. doi:10.1111/j.1600-0501.2012.02541.x.

[21] Y.-T. Xu, Q. Wu, Y.-M. Chen, R.J. Smales, S.-Y. Shi, M.-T. Wang, Antimicrobial effects of a bioactive glass combined with fluoride or triclosan on Streptococcus mutans biofilm., Arch. Oral Biol. 60 (2015) 1059–1065. doi:10.1016/j.archoralbio.2015.03.007.

[22] Y.L. Zhou, J. Chang, Study on Gentamicin Loading and Release from Mesoporous Bioactive Glasses (MBGs) with Different Shapes, Chemical Composition and Surface Property, J. Biomater. Tissue Eng. 2 (2012) 177–183. doi:10.1166/jbt.2012.1038.

[23] X. Zhang, W.-T. Jia, Y.-F. Gu, C.-Q. Zhang, W.-H. Huang, D.-P.

Wang, Borate bioglass based drug delivery of teicoplanin for treating osteomyelitis, Wuji Cailiao Xuebao/Journal Inorg. Mater. 25 (2010) 293–298. doi:10.3724/SP.J.1077.2010.00293.

[24] S.K. Nandi, B. Kundu, P. Mukherjee, T.K. Mandal, S. Datta, D.K. De, et al., In vitro and in vivo release of cefuroxime axetil from bioactive glass as an implantable delivery system in experimental osteomyelitis, Ceram. Int. 35 (2009) 3207–3216. doi:10.1016/j.ceramint.2009.05.005.

[25] Z. Xie, X. Liu, W. Jia, C. Zhang, W. Huang, [Vancomycin-loaded bioactive borate glass for treatment of chronic osteomyelitis in rabbits]., Zhongguo Xiu Fu Chong Jian Wai Ke Za Zhi. 25 (2011) 830–836. http://www.scopus.com/inward/record.url?eid=2-s2.0-84859894925&partnerID=tZOtx3y1.

[26] E. Vanea, S. Cavalu, F. Bănică, Z. Benyey, G. Göller, V. Simon, Adsorption and release studies of tetracycline from a bioactive glass, Stud. Univ. Babes-Bolyai Chem. (2011) 239–246. http://www.scopus.com/inward/record.url?eid=2-s2.0-84855268676&partnerID=40&md5=e47ba7dc6fbe80733da450742a2c5bdc.

[27] M.E. Olson, H. Ceri, D.W. Morck, A.G. Buret, R.R. Read, Biofilm bacteria: Formation and comparative susceptibility to antibiotics, Can. J. Vet. Res. 66 (2002) 86–92.

[28] M. Prabhu, S. Ruby Priscilla, K. Kavitha, P. Manivasakan, V. Rajendran, P. Kulandaivelu, In Vitro Bioactivity and Antimicrobial Tuning of Bioactive Glass Nanoparticles Added with Neem (Azadirachta indica) Leaf Powder, Biomed Res. Int. 2014 (2014) 1–10. doi:10.1155/2014/950691.

[29] R.F.A. Bonfim, V.R. Chitarra, R.T. Gomes, R.D. Zacarias, V.R. Santos, W.A. Vasconcelos, Antimicrobial activity of bioactive glass associated to Brazilian red and green propolis, Planta Med. 75 (2009) 1078.

[30] M. Cazzola, I. Corazzari, E. Prenesti, E. Bertone, E. Vernè, S. Ferraris, Bioactive glass coupling with natural polyphenols: Surface modification, bioactivity and anti-oxidant ability, Appl. Surf. Sci. 367 (2016) 237–248. doi:10.1016/j.apsusc.2016.01.138.

[31] L. Grenho, J. Barros, C. Ferreira, V.R. Santos, F.J. Monteiro,

M.P. Ferraz, et al., In vitro antimicrobial activity and biocompatibility of propolis containing nanohydroxyapatite, Biomed. Mater. 10 (2015) 25004. doi:10.1088/1748-6041/10/2/025004.

[32]   G.G. Mori, S. da S. Rodrigues, S.T. Shibayama, M. Pomini, C.O.F. do Amaral, Biocompatibility of a calcium hydroxide-propolis experimental paste in rat subcutaneous tissue., Braz. Dent. J. 25 (2014) 104–8. http://www.ncbi.nlm.nih.gov/pubmed/25140713 (accessed September 18, 2016).

[33]   J.M. Sforcin, Biological Properties and Therapeutic Applications of Propolis., Phytother. Res. 30 (2016) 894–905. doi:10.1002/ptr.5605.

[34]   A. Occhipinti, A. Germano, M.E. Maffei, Prevention of Urinary Tract Infection with Oximacro, A Cranberry Extract with a High Content of A-Type Proanthocyanidins: A Pre-Clinical Double-Blind Controlled Study., Urol. J. 13 (2016) 2640–9. http://www.ncbi.nlm.nih.gov/pubmed/27085566 (accessed April 15, 2017).

[35]   Y. Tao, P.A. Pinzón-Arango, A.B. Howell, T.A. Camesano, Oral consumption of cranberry juice cocktail inhibits molecular-scale adhesion of clinical uropathogenic Escherichia coli., J. Med. Food. 14 (2011) 739–45. doi:10.1089/jmf.2010.0154.

[36]   D. Kim, G. Hwang, Y. Liu, Y. Wang, A.P. Singh, N. Vorsa, et al., Cranberry Flavonoids Modulate Cariogenic Properties of Mixed-Species Biofilm through Exopolysaccharides-Matrix Disruption., PLoS One. 10 (2015) e0145844. doi:10.1371/journal.pone.0145844.

[37]   H. Koo, S. Duarte, R.M. Murata, K. Scott-Anne, S. Gregoire, G.E. Watson, et al., Influence of Cranberry Proanthocyanidins on Formation of Biofilms by Streptococcus mutans on Saliva-Coated Apatitic Surface and on Dental Caries Development in vivo, Caries Res. 44 (2010) 116–126. doi:10.1159/000296306.

[38]   G. Feng, M.I. Klein, S. Gregoire, A.P. Singh, N. Vorsa, H. Koo, The specific degree-of-polymerization of A-type proanthocyanidin oligomers impacts Streptococcus mutans glucan-mediated adhesion and transcriptome responses within

biofilms, Biofouling. 29 (2013) 629–640.
doi:10.1080/08927014.2013.794456.

[39] T. Kokubo, H. Takadama, How useful is SBF in predicting in vivo bone bioactivity?, Biomaterials. 27 (2006) 2907–2915. doi:10.1016/j.biomaterials.2006.01.017.

[40] A.L.B. Macon, T.B. Kim, E.M. Valliant, K. Goetschius, R.K. Brow, D.E. Day, et al., A unified in vitro evaluation for apatite-forming ability of bioactive glasses and their variants, J. Mater. Sci. Mater. Med. 26 (2015) 115. doi:10.1007/s10856-015-5403-9.

[41] Y.-Z. Liu, Y. Li, X.-B. Yu, L.-N. Liu, Z.-A. Zhu, Y.-P. Guo, Drug delivery property, bactericidal property and cytocompatibility of magnetic mesoporous bioactive glass., Mater. Sci. Eng. C. Mater. Biol. Appl. 41 (2014) 196–205. doi:10.1016/j.msec.2014.04.037.

[42] S. Lowel, J. Shields, M. Thomas, M. Thommes, Characterization of Porous Solids and Powders: Surface Area, Pore size and density, Springer s, Kluwer Academic Publishers, Dordrecht, 2004.

[43] G.A. Stanciu, I. Sandulescu, B. Savu, S.G. Stanciu, K.M. Paraskevopoulos, X. Chatzistavrou, et al., Investigation of the Hydroxyapatite Growth on Bioactive Glass Surface, J. Biomed. Pharm. Eng. 1 (2007) 34–39. http://citeseerx.ist.psu.edu/viewdoc/download?doi=10.1.1.502.89 02&rep=rep1&type=pdf (accessed April 30, 2017).

[44] S.-J. Shih, W.-L. Tzeng, R. Jatnika, C.-J. Shih, K.B. Borisenko, Control of Ag nanoparticle distribution influencing bioactive and antibacterial properties of Ag-doped mesoporous bioactive glass particles prepared by spray pyrolysis, J. Biomed. Mater. Res. - Part B Appl. Biomater. 103 (2014) 899–907. doi:10.1002/jbm.b.33273.

[45] V. Anand, K.J. Singh, K. Kaur, Evaluation of zinc and magnesium doped 45S5 mesoporous bioactive glass system for the growth of hydroxyl apatite layer, J. Non. Cryst. Solids. 406 (2014) 88–94. doi:10.1016/j.jnoncrysol.2014.09.050.

[46] J. Hum, A.R. Boccaccini, Bioactive glasses as carriers for bioactive molecules and therapeutic drugs: A review, J. Mater. Sci. Mater. Med. 23 (2012) 2317–2333. doi:10.1007/s10856-012-

4580-z.

[47] M. Manzano, M. Vallet-Regí, New developments in ordered mesoporous materials for drug delivery, J. Mater. Chem. 20 (2010) 5593–5604. doi:10.1039/b922651f.

[48] N. Letaïef, A. Lucas-Girot, H. Oudadesse, R. Dorbez-Sridi, P. Boullay, Investigation of the surfactant type effect on characteristics and bioactivity of new mesoporous bioactive glass in the ternary system SiO 2-CaO-P2O5: Structural, textural and reactivity studies, Microporous Mesoporous Mater. 195 (2014) 102–111. doi:10.1016/j.micromeso.2014.03.035.

[49] Y.F. Goh, A.Z. Alshemary, M. Akram, M.R.A. Kadir, R. Hussain, Bioactive Glass: An In-Vitro Comparative Study of Doping with Nanoscale Copper and Silver Particles, Int. J. Appl. Glas. Sci. 5 (2014) 255–266. doi:10.1111/ijag.12061.

[50] Y.F. Zhu, S. Kaskel, Comparison of the in vitro bioactivity and drug release property of mesoporous bioactive glasses (MBGs) and bioactive glasses (BGs) scaffolds, Microporous Mesoporous Mater. 118 (2009) 176–182. doi:10.1016/j.micromeso.2008.08.046.

[51] W. Xia, J. Chang, Preparation, in vitro bioactivity and drug release property of well-ordered mesoporous 58S bioactive glass, J. Non. Cryst. Solids. 354 (2008) 1338–1341. doi:10.1016/j.jnoncrysol.2006.10.084.

[52] X. Zhang, D. Zeng, N. Li, J. Wen, X. Jiang, C. Liu, et al., Functionalized mesoporous bioactive glass scaffolds for enhanced bone tissue regeneration, Sci. Rep. 6 (2016) 19361. doi:10.1038/srep19361.

[53] H. Wang, S. Zhao, X. Cui, Y. Pan, W. Huang, S. Ye, et al., Evaluation of three-dimensional silver-doped borate bioactive glass scaffolds for bone repair: Biodegradability, biocompatibility, and antibacterial activity, J. Mater. Res. 30 (2015) 2722–2735. doi:10.1557/jmr.2015.243.

[54] D. Arcos, J. Peña, M. Vallet-Regí, Influence of a SiO2-CaO-P2O5 Sol-Gel Glass on the Bioactivity and Controlled Release of Ceramic/Polymer/Antibiotic Mixed Materials, Chem. Mater. 15 (2003) 4132–4138. doi:10.1021/cm031074n.

[55] W. Xia, J. Chang, Well-ordered mesoporous bioactive glasses (MBG): A promising bioactive drug delivery system, J. Control. Release. 110 (2006) 522–530. doi:10.1016/j.jconrel.2005.11.002.

[56] S.-J. Shih, W.-L. Tzeng, R. Jatnika, C.-J. Shih, K.B. Borisenko, Control of Ag nanoparticle distribution influencing bioactive and antibacterial properties of Ag-doped mesoporous bioactive glass particles prepared by spray pyrolysis., J. Biomed. Mater. Res. B. Appl. Biomater. 103 (2015) 899–907. doi:10.1002/jbm.b.33273.

[57] Y.F. Goh, A.Z. Alshemary, M. Akram, M.R. Abdul Kadir, R. Hussain, In-vitro characterization of antibacterial bioactive glass containing ceria, Ceram. Int. 40 (2014) 729–737. doi:10.1016/j.ceramint.2013.06.062.

[58] L. Drago, D. Romanò, E. De Vecchi, C. Vassena, N. Logoluso, R. Mattina, et al., Bioactive glass BAG-S53P4 for the adjunctive treatment of chronic osteomyelitis of the long bones: an in vitro and prospective clinical study., BMC Infect. Dis. 13 (2013) 584. doi:10.1186/1471-2334-13-584.

[59] D.C. Coraca-Huber, M. Fille, J. Hausdorfer, D. Putzer, M. Nogler, Efficacy of antibacterial bioactive glass S53P4 against S. aureus biofilms grown on titanium discs in vitro., J. Orthop. Res. 32 (2014) 175–177. doi:10.1002/jor.22463.

[60] N.C. Lindfors, Bioactive glass S53P4 as a bone graft substitute in the treatment of osteomyelitis, Bioact. Glas. Mater. Prop. Appl. 47 (2011) 209–216. doi:10.1016/B978-1-84569-768-6.50009-0.

[61] G.M. De Souza, Nanoparticles in restorative materials, in: Nanotechnol. Endod. Curr. Potential Clin. Appl., Springer International Publishing, Clinical Sciences Department, Faculty of Dentistry, University of Toronto, 124 Edward St, Toronto, ON, Canada, 2015: pp. 139–172. doi:10.1007/978-3-319-13575-5_8.

[62] J.B. Blumberg, T.A. Camesano, A. Cassidy, P. Kris-Etherton, A. Howell, C. Manach, et al., Cranberries and Their Bioactive Constituents in Human Health, Adv. Nutr. An Int. Rev. J. 4 (2013) 618–632. doi:10.3945/an.113.004473.

[63] T.S. Jafarzadeh Kashi, R. Kasra Kermanshahi, M. Erfan, E. Vahid Dastjerdi, Y. Rezaei, F.S. Tabatabaei, Evaluating the in-vitro antibacterial effect of Iranian propolis on oral microorganisms, Iran. J. Pharm. Res. 10 (2011) 363–368.

CAPÍTULO III

5 CONSIDERAÇÕES FINAIS

O biovidro ativo tem sido desenvolvido para diversas aplicações nos processos de reparo e tratamento de infecção óssea. No em tanto, o biovidro ativo tem suas limitações para o tratamento de infecções nos leitos receptores que têm como fator causal a aderência do biofilme multi-espécies. Consequentemente a engenharia tecidual tem modificado o biovidro ativo incorporando na sua estrutura tanto química como física agentes anti-biofilme orgânicos e inorgânicos. Nos últimos anos, as diferentes moléculas derivadas de óxidos de metal, antibióticos e outros agentes sintéticos incorporadas no biovidro ativo têm dado resultados satisfatórios antimicrobianos, mas não têm apresentado resultados concluintes com respeito à inibição do biofilme. Assim, o presente trabalho explorou o estado da arte do tema para desenvolver assim partículas do biovidro ativo 58S normal e mesoporoso incorporando moléculas de brometo, cranberry e própolis a fim de combater as infeções ósseas associadas ao biofilme. Em princípio, o biovidro ativo 58S incorporando brometo mostrou resultados promissórios com relação a inibição de biofilme oral multi-especies. Por outro lado, o biovidro mesoporoso incorporando as moléculas naturais mostrou uma alta bioatividade que é uma característica inerente do biomaterial, sendo assim um material promissório que poderia atuar como sistema de liberação localizado de agentes anti-biofilme no leito receptor. Contudo, futuros estudos são necessários para estabelecer os agentes anti-biofilme mais efetivos para tratar as infeções ósseas que possam ser incorporados no biovidro ativo sem interferir com sua bioatividade inerente, nem causar efeitos citotóxicos no leito receptor.

6 REFERÊNCIAS

ALLAN, I.; NEWMAN, H.; WILSON, M. Particulate Bioglass reduces the viability of bacterial biofilms formed on its surface in an in vitro model. **Clinical oral implants research**, v. 13, n. 1, p. 53–58, fev. 2002.

AMINI, A. R.; LAURENCIN, C. T.; NUKAVARAPU, S. P. Bone tissue engineering: recent advances and challenges. **Critical reviews in biomedical engineering**, v. 40, n. 5, p. 363–408, 2012.

BELLANTONE, M.; COLEMAN, N. J.; HENCH, L. L. A novel sol-gel derived bioactive glass featuring antibacterial properties. In: GIANNINI, S.; MORONI, A. (Eds.). . **Bioceramics**. Key Engineering Materials. Univ London Imperial Coll Sci Technol & Med, Dept Mat, London SW7 2BP, England. Bellantone, M (reprint author), Univ London Imperial Coll Sci Technol & Med, Dept Mat, Prince Consort Rd, London SW7 2BP, England.: Trans Tech Publications Ltd, 2000. v. 192–1p. 597–600.

CABRAL DA CRUZ, A. C. et al. Utilização de vidros bioativos como substitutos ósseos: Revisão de literatura. **Revista de Odontologia da Universidade Cidade de São Paulo**, v. 18, n. 3, p. 287–295, 2006.

DAVIES, D. Understanding biofilm resistance to antibacterial agents. **Nature reviews. Drug discovery**, v. 2, n. 2, p. 114–22, 2003.

DOMINGUES, Z. R. et al. Bioactive glass as a drug delivery system of tetracycline and tetracycline associated with beta-cyclodextrin. **Biomaterials**, v. 25, n. 2, p. 327–333, jan. 2004.

EL-GHANNAM, A.; AHMED, K.; OMRAN, M. Nanoporous delivery system to treat osteomyelitis and regenerate bone: Gentamicin release kinetics and bactericidal effect. **Journal of Biomedical Materials Research Part B-Applied Biomaterials**, v. 73B, n. 2, p. 277–284, 2005.

EL-KADY, A. M. et al. Synthesis, characterization and microbiological response of silver doped bioactive glass nanoparticles. **Ceramics International**, v. 38, n. 1, p. 177–188, jan. 2012.

GALARRAGA-VINUEZA, M. E. et al. Anti-biofilm properties of bioactive glasses embedding organic active compounds. **Journal of Biomedical Materials Research Part A**, nov. 2016.

GALARRAGA-VINUEZA, M. E. et al. Inhibition of multi-species oral biofilm by bromide doped bioactive glass. **Journal of Biomedical Materials Research Part A**, 6 abr. 2017.

HENCH, L. L. The story of Bioglass®. **Journal of Materials Science: Materials in Medicine**, v. 17, n. 11, p. 967–978, 2006.

HOPPE, A.; GÜLDAL, N. S.; BOCCACCINI, A. R. A review of the biological response to ionic dissolution products from bioactive glasses and glass-ceramics. **Biomaterials**, v. 32, n. 11, p. 2757–2774, 2011.

HUM, J.; BOCCACCINI, A. R. Bioactive glasses as carriers for bioactive molecules and therapeutic drugs: A review. **Journal of Materials Science: Materials in Medicine**, v. 23, n. 10, p. 2317–2333, 2012.

JIA, W.-T. et al. Novel borate glass/chitosan composite as a delivery vehicle for teicoplanin in the treatment of chronic osteomyelitis. **Acta biomaterialia**, v. 6, n. 3, p. 812–819, mar. 2010.

JONES, J. R. Review of bioactive glass: from Hench to hybrids. **Acta biomaterialia**, v. 9, n. 1, p. 4457–86, 2013.

KRISHNAN, V.; LAKSHMI, T. Bioglass: A novel biocompatible innovation. **Journal of Advanced Pharmaceutical Technology and Research**, v. 4, n. 2, p. 78–83, 2013.

LI, Y. et al. Mesoporous bioactive glass as a drug delivery system: fabrication, bactericidal properties and biocompatibility. **Journal of materials science. Materials in medicine**, v. 24, n. 8, p. 1951–1961, ago. 2013.

MABROUK, M. et al. Effect of ciprofloxacin incorporation in PVA and PVA bioactive glass composite scaffolds. **Ceramics International**, v. 40, n. 3, p. 4833–4845, abr. 2014.

MALAVASI, G. et al. **Novel smart bio-nanomaterials: Bioactive glasses containing metal nano-particles conjugated with molecules of biological interest**Technical Proceedings of the 2012 NSTI Nanotechnology Conference and Expo, NSTI-Nanotech 2012. **Anais**...2012Disponível em: <http://www.scopus.com/inward/record.url?eid=2-s2.0-84865036964&partnerID=tZOtx3y1>

MIOLA, M. et al. Antibiotic loading on bioactive glasses and glass-ceramics: an approach to surface modification. **Journal of biomaterials**

applications, v. 28, n. 2, p. 308–319, ago. 2013.

PRABHU, M. et al. In Vitro Bioactivity and Antimicrobial Tuning of Bioactive Glass Nanoparticles Added with Neem (Azadirachta indica) Leaf Powder. **BioMed Research International**, v. 2014, p. 1–10, 2014.

RIVADENEIRA, J. et al. Evaluation of antibacterial and cytotoxic effects of nano-sized bioactive glass/collagen composites releasing tetracycline hydrochloride. **Journal of applied microbiology**, v. 116, n. 6, p. 1438–1446, jun. 2014.

RIVADENEIRA, J. et al. Evaluation of the antibacterial effects of vancomycin hydrochloride released from agar-gelatin-bioactive glass composites. **Biomedical materials (Bristol, England)**, v. 10, n. 1, p. 15011, fev. 2015.

STEVANOVIĆ, M. et al. 45S5Bioglass®-based scaffolds coated with selenium nanoparticles or with poly(lactide-co-glycolide)/selenium particles: Processing, evaluation and antibacterial activity. **Colloids and surfaces. B, Biointerfaces**, v. 132, p. 208–15, 1 ago. 2015.

XIA, W. et al. The pH-controlled dual-drug release from mesoporous bioactive glass/polypeptide graft copolymer nanomicelle composites. **European journal of pharmaceutics and biopharmaceutics : official journal of Arbeitsgemeinschaft fur Pharmazeutische Verfahrenstechnik e.V**, v. 69, n. 2, p. 546–552, jun. 2008.

XIA, W.; CHANG, J. Well-ordered mesoporous bioactive glasses (MBG): A promising bioactive drug delivery system. **Journal of Controlled Release**, v. 110, n. 3, p. 522–530, 2006.

XIE, Z. et al. Treatment of osteomyelitis and repair of bone defect by degradable bioactive borate glass releasing vancomycin. **Journal of controlled release : official journal of the Controlled Release Society**, v. 139, n. 2, p. 118–126, out. 2009a.

XIE, Z.-P. et al. In vivo study effect of particulate Bioglass® in the prevention of infection in open fracture fixation. **Journal of Biomedical Materials Research - Part B Applied Biomaterials**, v. 90, n. 1, p. 195–201, 2009b.

XU, Y.-T. et al. Antimicrobial effects of a bioactive glass combined with fluoride or triclosan on Streptococcus mutans biofilm. **Archives of Oral Biology**, v. 60, n. 7, p. 1059–1065, 2015.

YAO, Q. Q. et al. Bioglass (R)-based scaffolds incorporating

polycaprolactone and chitosan coatings for controlled vancomycin delivery. **Ceramics International**, v. 39, n. 7, p. 7517–7522, 2013.